ISSN 1075-7015, Geology of Ore Deposits, 2006, Vol. 48, No. 1, pp. 1–22. © Pleiades Publishing, Inc., 2006.
Original Russian Text © N.S. Bortnikov, 2006, published in Geologiya Rudnykh Mestorozhdenii, 2006, Vol. 48, No. 1, pp. 3–28.

Geochemistry and Origin of the Ore-Forming Fluids in Hydrothermal–Magmatic Systems in Tectonically Active Zones

N. S. Bortnikov

Institute of Geology of Ore Deposits, Petrography, Mineralogy, and Geochemistry, Russian Academy of Sciences, Staromonetnyi per. 35, Moscow, 119017 Russia

Received April 25, 2005

Abstract—Data on fluid inclusions and stable isotope compositions (O, H, C, and S) in minerals have been summarized for large- and middle-scale mesothermal gold deposits (Nezhdaninsk, Berezovsk, Kochkar', Svetlinsk, Darasun, and Maisk), cassiterite–silicate–sulfide deposits of Sikhote Alin (Solnechnoe, Arsen'evsk, and Vysokogorsk), vein silver–base metal deposits in the Southern Verkhoyansk region (Prognoz and Kupol'noe), and epithermal copper–bismuth–silver–base metal deposits of the Karamazar district in Tajikistan (Kanimansur, Tary Ekan, and Zambarak). It is shown that ores precipitated from fluids with salinity varying from brines (up to 60 wt % NaCl equiv) to dilute fluids (1–3 wt % NaCl equiv). As a rule, fluids of different compositions entered the hydrothermal–magmatic system. A fluid mixture of H_2O–CO_2–NaCl ± CH_4 ± N_2 predominated in the orogenic (mesothermal) gold-bearing hydrothermal systems, with deposition of the final-stage gold-bearing sulfosalts from aqueous–salt fluid. Brines played a significant role in the formation of cassiterite–silicate–sulfide and vein silver–base metal deposits. The brines often coexisted with a low-density vapor-rich fluid at the ore deposition site. The obtained data suggest a predominant magmatic component in the hydrothermal–magmatic systems, with a significant contribution of meteoric waters.

DOI: 10.1134/S1075701506010016

INTRODUCTION

The most important problems in study of ore deposits are the conditions of formation and origin of ore-forming fluids, the sources of ore metals and their transportation by hydrothermal fluids to deposition sites, and the causes of their precipitation. The most intense fluid flows occur along high-permeability zones, as distinctly recognized from the development of abundant metasomatic halos around them. The fluid regime in the Earth's crust plays an important role in the accumulation of metals in fault zones, affects the geochemical composition of the Earth's crust through fluid interaction with host rocks along infiltration zones, and controls migration of components. However, concepts of the origin and compositions of ore-bearing fluids are still debated. Special attention has been paid to the role of magmatic and meteoric fluids. This problem has been discussed for many centuries. Agricola (1494–1555) was the first who supposed that heated meteoric waters circulating at deep levels of the Earth's crust leached metals from rocks and transported them to the ore precipitation site. Decartes (1596–1650) hypothesized that gases exsolving from a melt during crystallization can transfer metals and precipitate them in fractures. From that time on, the discussion on the role of magmatic and meteoric fluid has not ceased.

The composition and nature of ore-forming fluids are not only of scientific interest but also play a significant role in understanding ore-forming processes and choosing a strategy for ore prospecting. Recent studies (Borisenko, 1977; Bortnikov *et al.*, 1996, 1998, 1999, 2004; Prokof'ev *et al.*, 2000; Safonov *et al.*, 2000a, 2000b; Ridley and Dimond, 2000; Roedder, 1984; and others) have provided a great deal of information on the chemical and isotope composition of fluids that precipitated ores in different geodynamic settings: mesothermal gold deposits of fold zones, suprasubduction cassiterite–silicate–sulfide deposits, and epithermal deposits of continental volcanic belts. This paper summarizes the studies of the composition and origin of ore-forming fluid in different geodynamic settings that were carried out by the author or under his leadership in the last decade.

Address for correspondence: N.S. Bortnikov. E-mail: bns@igem.ru

MESOTHERMAL GOLD DEPOSITS

Mesothermal gold deposits are ore deposits that formed under relatively high pressures (1–3 kbar) and temperatures (200–400°C) (Ridley and Dimond, 2000). The mesothermal deposits were recently included in the group of orogenic gold deposits that formed in convergent margin settings during accretion or collision of terranes owing to plate subduction and/or lithospheric lamination (Groves *et al.*, 1998, 2005). The orogenic deposits typically form at the final stages of tectonomagmatic and metamorphic evolution of the orogen (Groves *et al.*, 2005).

Table 1. Characteristics of studied gold deposits

Deposit	Host rocks	Magmatic rock associations	Ore morphology	Wall rock alteration	Main ore minerals	Age, Ma
Svetlinsk, Urals	Paleozoic volcanosedimentary and magmatic rocks	Plagiogranites and granodiorites	Veins and veinlets	Quartz–sericite–carbonate and chlorite–carbonate–talc rocks	Pyrite; pyrrhotite; chalcopyrite; galena; Au; tellurides of Au, Ni, Fe, Pb	350
Berezovsk, Urals	Volcanosedimentary rocks, granite porphyry dikes	Granite porphyries	Veins and veinlets	Quartz–orthoclase–carbonate, quartz–sericite–carbonate, and chlorite–carbonate–talc rocks	Scheelite, pyrite, arsenopyrite, galena, Au, minerals of Bi, sphalerite, carbonates	364
Kochkar', Urals	Early Carboniferous granodiorite–adamellite intrusion	Granites and leucogranites	Veins and stockworks	Quartz–sericite–carbonate and chlorite–carbonate–talc rocks	Quartz, pyrite, arsenopyrite, Au, tellurides of Au, Bi sulfosalts, stibnite, carbonates	Postore metamorphism 260
Olimpiada, Yenisei Range	Lower Riphean schists	Granites	Lenses and zones of disseminated mineralization	Mica–quartz–zoisite and zoisite–quartz metasomatites	Quartz, scheelite, zoisite, arsenopyrite, pyrrhotite, Au, stibnite, berthierite, carbonates	856–792
Darasun, Transbaikal region	Middle Paleozoic–Early Mesozoic gabbroids and granitoids	Alkali subvolcanic granodiorite porphyries	Veins and mineralized brecciation zones	Propylites, quartz–sericite–carbonate and chlorite–carbonate–talc rocks	Quartz; tourmaline; pyrite; arsenopyrite; chalcopyrite; galena; Au; tellurides of Au, Ag, and Bi; carbonates	150–144
Maisk, Chukotka	Triassic organic-rich sedimentary rocks	Granodiorite porphyries	Veins, veinlets, and disseminated ores	Quartz–sericite–carbonate and quartz–sericite metasomatites	Quartz, pyrite, arsenopyrite, cassiterite, stannite, Au, tellurides of Bi, stibnite	118–64
Nezhdaninsk, Yakutia	Permian sedimentary rocks	Granodiorites, leucogranites	Veins, veinlets, and disseminated ores	Propylites, sericite–carbonate and quartz–sericite–carbonate rocks	Quartz, pyrite, arsenopyrite, Au, sulfosalts of Ag, carbonates	154–94

Mesothermal gold deposits of different age and geographic position share common features: (1) they are confined to orogenic belts composed of terrigenous or volcano-terrigenous sequences that were regionally metamorphosed, folded, and cut by granite intrusions; (2) geophysical data indicate the existence of deep-seated granite batholiths beneath the hydrothermal systems; (3) host rocks experienced contact metamorphism; (4) ore-controlling structures are regional faults; and (5) gold veins postdate metamorphism and emplacement of granitoids. Several conceptual models have been proposed to explain the origin of these deposits. They suggest a genetic relation of the ore formation with sedimentation and regional metamorphism, granulitization, and emplacement of intrusions of different composition (tonalite–granodiorite, oxidized felsitic magmas, and lamprophyres) (Groves *et al.*, 1998; Hageman and Cassidy, 2000; Kerrich, 1990). The generally accepted viewpoint suggests that mineral-forming fluid originated by decarbonatization and dehydration during regional metamorphism. This viewpoint is supported by most North American and Australian geologists and geochemists. It is believed to be well consistent with data on stable isotopes, fluid inclusions, and REE and LILE distributions (Kerrich, 1990).

Below, data on fluid inclusions and stable isotopes in minerals from the Nezhdaninsk, Maisk, Darasun, Svetlinsk, Berezovsk, and Kochkar' deposits are summarized. These deposits are briefly characterized in Table 1; more detailed data on the geology, sequence of mineral formation, and fluid regime were previously reported in (Bortnikov *et al.*, 1998, 1999, 2004; Prokof'ev *et al.*, 2000).

Fluid Inclusions

In terms of phase composition at room temperature, four types of fluid inclusions were identified in quartz from mesothermal deposits (Fig. 1): (1) two-phase fluid inclusions consisting of aqueous (low-salinity) solution with a vapor bubble (Fig. 1a); (2) inclusions consisting of aqueous solution and liquid and (not universally) carbonic acid vapor (occasionally with significant CH_4 and N_2 impurities) (Fig. 1b); (3) vapor-rich inclusions consisting of predominant CO_2 with occasional CH_4

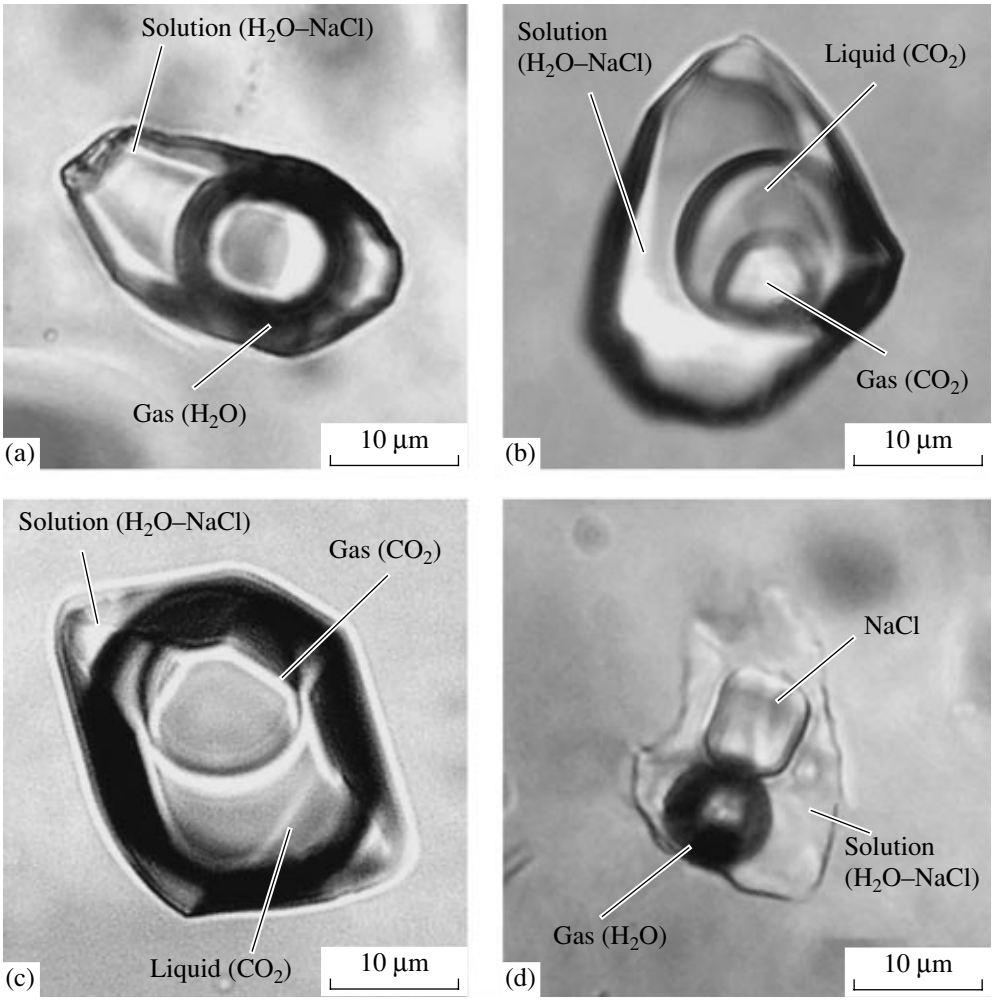

Fig. 1. Types of fluid inclusions in the minerals of studied mesothermal gold deposits. (a) Two-phase inclusion of diluted solution; (b) CO_2–aqueous inclusion of vapor-rich fluid; (c) vapor-rich inclusion; (d) multiphase inclusion of chloride brine (images of V.Yu. Prokof'ev).

and N_2 (Fig. 1c); and (4) multiphase inclusions of chloride solutions with a vapor bubble, aqueous solution, and cubic isotropic chloride crystals (Fig. 1d). It should be noted that not all types of fluid inclusions were found at all deposits.

These findings indicate that mineral assemblages of the mesothermal deposits formed from fluids of different composition (Table 2, Fig. 2). These are H_2O–CO_2–NaCl ± CH_4 ± N_2 fluid, vapor-rich fluid consisting of dense CO_2 with trace NH_4 and N_2, brines, and low- to moderate-salinity aqueous fluids. The interpretation of the fluid inclusion study is not unambiguous. It is difficult to ascertain which of the found fluids is gold-bearing. At room temperature, quartz from gold veins contains fluid inclusions consisting of aqueous solution and liquid and, in some cases, CO_2 vapor (occasionally with trace CH_4 and N_2), as well as vapor-rich inclusions consisting of predominant CO_2 with occasional CH_4 and N_2. These fluids played the main role in the formation of gold-bearing quartz bodies. Since these fluid inclusions are syngenetic, liquid bicarbonate–aqueous–salt and vapor-rich fluid formed due immiscibility of H_2O–CO_2–NaCl ± CH_4 ± N_2 protofluid with a temperature and pressure drop (Bortnikov *et al.*, 1996, 2004). The vapor-rich aqueous–salt fluid contains dissolved chlorides (16.8–1.2 wt % NaCl equiv). The salinity of the ore fluids at the studied deposits was different (Table 2, Fig. 2). The fluids also were high in dissolved gases (33.4–1.0 wt %). In addition to CO_2, they contained dissolved CH_4 (Olimpiada, Maisk, and Nezhdaninsk) or N_2 (Svetlinsk). Sodium predominated over potassium among cations, and Cl^- over HCO_3^- among anions.

The vapor-rich ore-forming fluids contain dense CO_2, occasionally with trace N_2 (the Berezovsk and Svetlinsk deposits) or CH_4 (the Maisk deposit). Purely CH_4 fluids were found at the Nezhdaninsk deposit, while vapor inclusions with variable proportions of a triple CO_2–CH_4–N_2 mixture up to pure gases were found at the Olimpiada deposit.

Table 2. Main deposition parameters of the large mesothermal gold deposits of Russia

Deposit	Fluid	Main components	n	T_{hom}, °C	C_{salt}, wt % NaCl equiv	$CO_2 \pm N_2 \pm CH_4$, wt %	P, bar	$\frac{P_{tot}}{P_{H_2O}}$
Svetlinsk, Urals	Vapor-rich solution	$H_2O + CO_2 + NaCl$	89	405–255	16.8–6.6	33.4–3.5	3660–1020	48.3–6.8
	Vapor	$CO_2 \pm N_2$	656	–	–	95–70		
	Aqueous solution	$H_2O + NaCl$	115	310–130	19.8–4.8	2–0	–	–
Berezovsk, Urals	Vapor-rich solution	$H_2O + CO_2 + NaCl$	380	365–255	14.9–2.0	27.7–10.6	3460–810	42.7–13.0
	Vapor	CO_2	816	–	–	98–86		
Kochkar, Urals	Vapor-rich solution	$H_2O + CO_2 + NaCl$	126	370–244	14.2–7.7	28.2–9.7	2580–450	22.7–3.8
	Vapor	CO_2	187	–	–	96–73		
	Aqueous solution	$H_2O + NaCl$	51	272–180	16.7–6.3	2–0	–	–
Olimpiada, Yenisei Range	Vapor-rich solution	$H_2O + NaCl$	434	485–190	17.8–2.4	6–1	2710–190	56.5–3.6
	Vapor	$CO_2 \pm N_2 \pm CH_4$	1361	–	–	98–86		
	Aqueous solution	$H_2O + NaCl$	273	335–105	25.0–1.2	2–0	–	–
Darasun, Transbaikal region	Brine	$H_2O + NaCl + CaCl_2$	54	445–265	52.6–30.5	2–1	2040–120	13.8–1.8
	Vapor-rich solution	$H_2O + NaCl$	235	430–160	22.8–2.2	9–1	1540–150	17.2–1.0
	Vapor	$H_2O + CO_2$	43	–	–	90–74		
	Aqueous solution	$H_2O + NaCl$	37	280–120	12.8–2.2	2–0	–	–
Maisk, Chukotka	Brine	$H_2O + NaCl + CaCl_2$	22	535–170	37.5–30.2	8–1	–	–
	Vapor-rich solution	$H_2O + CO_2 + NaCl$	127	430–238	8.8–2.2	22.9–7.0	1170–270	18.0–1.6
	Vapor	$CO_2 \pm CH_4$	103	–	–	92–75		
	Aqueous solution	$H_2O + NaCl$	130	287–119	10.1–0.7	3–1	–	–
Nezhdaninsk, Yakutia	Vapor-rich solution	$H_2O + CO_2 + NaCl$	330	387–249	9.6–1.2	31.7–8.4	1950–400	46.6–2.9
	Gas	$CO_2 \pm CH_4$	481	–	–	97–78		
	Aqueous solution	$H_2O + NaCl$	93	294–129	26.3–2.4	3–1	–	–
	Brine	$H_2O + NaCl + CaCl_2$	15	204–199	31.1–31.0	2–1	–	–

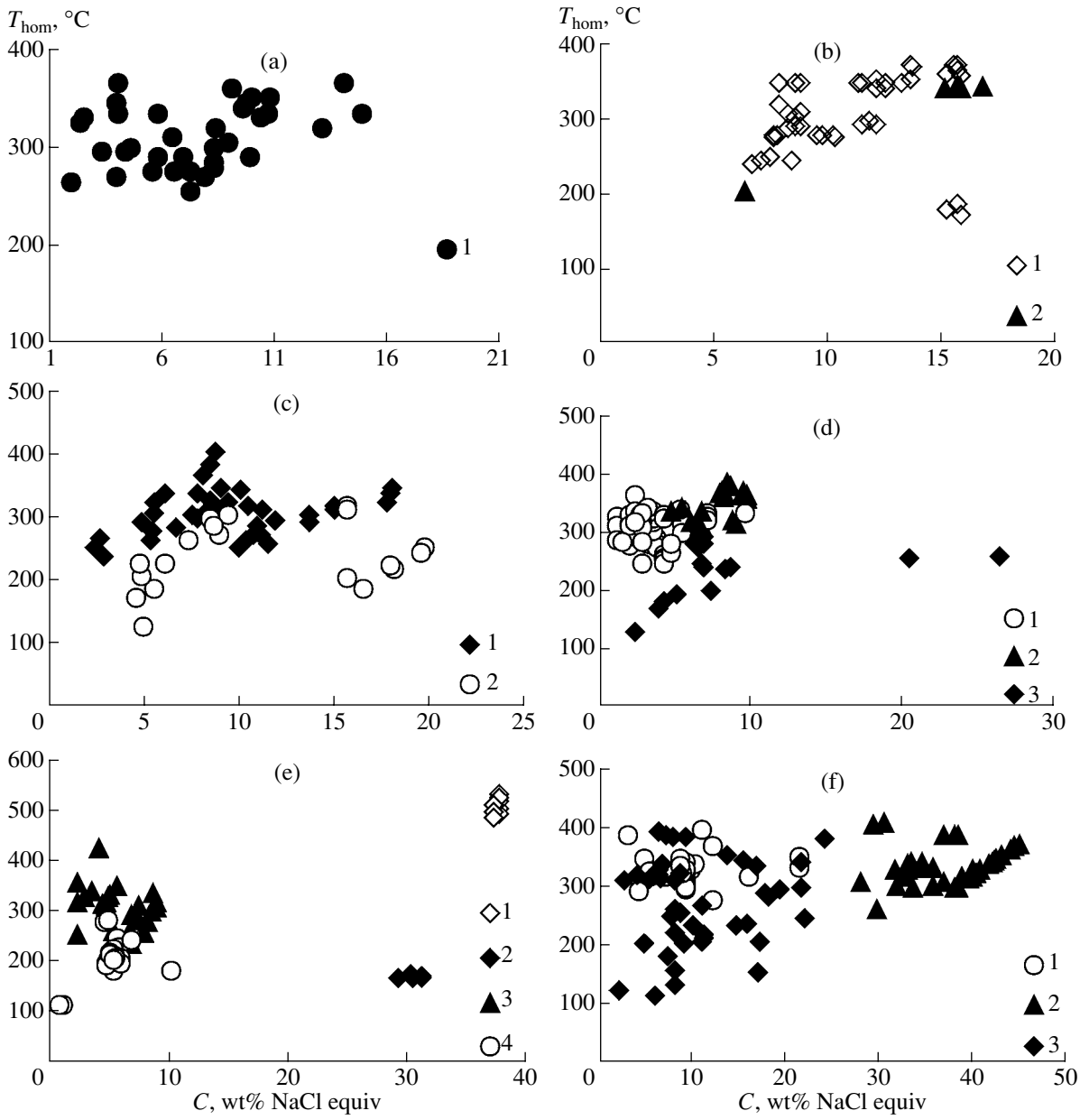

Fig. 2. Variations of homogenization temperature versus salinity of the fluid inclusions in quartz from the mesothermal Berezovsk (a), Kochkar' (b), Svetlinsk (c), Nezhdaninsk (d), Maisk (e), and Darasun (f) gold deposits. (a) Bicarbonate–aqueous liquid-rich inclusions; (b) (1) bicarbonate–aqueous liquid-rich inclusions, (2) aqueous–salt fluid inclusions; (c) (1) bicarbonate–aqueous liquid-rich fluid inclusions, (2) aqueous–salt fluid inclusions; (d) (1) gold–quartz assemblage, (2) quartz–rare metal assemblage, (3) silver–base metal assemblage; (e) (1, 2) high-salinity fluid inclusions, (3) bicarbonate–aqueous liquid-rich fluid inclusions, (4) aqueous–salt fluid inclusions; (f) (1) bicarbonate–aqueous liquid-rich fluid inclusions, (2) brines, (3) aqueous–salt fluid inclusions.

It should be noted that fluids of contrasting chemical and phase composition were involved in the mesothermal gold-forming hydrothermal–magmatic systems (Fig. 2, Table 2). Two ore-forming fluids were identified at the Berezovsk deposit (Fig. 2a): liquid bicarbonate–aqueous–salt with salinity from 26.3 to 0.7 wt % NaCl equiv, and vapor-rich (mainly CO_2) fluids, which formed through immiscibility of the H_2O–CO_2–NaCl fluid (Bortnikov *et al.*, 1999). Ores at the Svetlinsk and Kochkar deposits precipitated from a more complex fluid (Figs. 2b, 2c). Aqueous–salt fluid was found there in addition to bicarbonate–aqueous–salt fluid (with salinities from 8.8 to 16.8 wt % NaCl equiv and from 15.7 to 7.0 wt % NaCl equiv, respectively) and vapor-rich $CO_2 \pm CH_4$ fluid. The origin of this fluid is unclear. It could be derived during evolution of a protofluid H_2O–CO_2–NaCl $\pm$ CH_4 $\pm$ N_2 mixture or owing to input from a different source (Bortnikov *et al.*, 1996). Fluids having contrasting chemical and phase composition produced different ore mineral assemblages at the

Nezhdaninsk (Fig. 2d) and Maisk (Fig. 2e) deposits. Gold–quartz ores of the Nezhdaninsk deposit precipitated from a CO_2–H_2O fluid with salinity 9.6–1.2 wt % NaCl equiv, 7.2–3.0 mol/kg solution CO_2, and 1.0–0.5 mol/kg solution CH_4 at 368–267°C—and 1950–720 bar and from vapor-rich fluids consisting of dense (0.97–0.47 g/cm^3) CO_2 with trace (7–4 mol %) CH_4 and N_2. Crystal-like quartz in silver–base metal ore mineralization precipitated from CO_2–H_2O solutions within wide ranges of temperature (387–129°C) and pressure (1890–790 bar) at 8.6–2.4 wt % NaCl equiv, 3.9–0.1 mol/kg solution CO_2, and 1.6–0.5 mol/kg solution CH_4. Gold–rare metal ores in the outer contact of the Kurum massif formed from aqueous–salt fluids with 31.1–1.9 wt % NaCl equiv, 1.8–0 mol/kg solution CO_2, and 2.5–1.5 mol/kg solution CH_4 at 374–199°C and 630–570 bar (Bortnikov *et al.*, 1998). Ore-forming systems of the Maisk deposit involved three fluids differing in composition and physicochemical parameters (Bortnikov *et al.*, 2004). Gold–sulfide ores precipitated from H_2O–CO_2–CH_4 fluid with salinity 8.8–2.2 wt % NaCl equiv at 360–240°C and 1.1–0.9 kbar. Cassiterite–sulfide ore mineralization crystallized from high- (37.5–30.0 wt % NaCl equiv) and low-salinity fluids at 500–170°C. Quartz–stibnite ores formed from an aqueous fluid with salinity 10.1–0.7 wt % NaCl equiv at 250–120°C. Mineral assemblages of the Darasun deposit also formed from compositionally different fluids. Quartz phenocrysts in granodiorite porphyries contain mineral-forming brines with salinity 52.6–29.9 wt % NaCl equiv (Fig. 2f) (Prokof'ev *et al.*, 2000). Quartz in early-stage veins and metasomatites also precipitated from high-salinity fluids (44.8–30.5 wt % NaCl equiv). Carbonic acid was found only in low-saline fluid inclusions (often in quartz from quartz–sericite–carbonate rocks). Quartz from gold veins with base metal and sulfosalt mineralization crystallized from aqueous–salt fluids with salinity 22.2–4.8 wt % NaCl equiv. Minerals of the sulfostibnite and final stages (quartz and calcite) deposited from dilute aqueous–salt fluids with salinity 12.8–2.2 wt % NaCl equiv at 210–120°C.

Thus, the investigations showed that gold-bearing fluids of the studied mesothermal gold deposits contained solutions with significantly higher salinity as compared to orogenic deposits (Hageman and Cassidy, 2000; Ridley and Dimond, 2000). Brines and dilute aqueous–salt fluids, in addition to fluid H_2O–CO_2–$NaCl \pm CH_4 \pm N_2$ mixtures, contributed to mesothermal gold deposits. However, the main role in the formation of gold ore bodies was played by bicarbonate–aqueous–salt fluid.

Stable Oxygen and Hydrogen Isotopes

Oxygen isotope compositions of quartz of metasomatites and gold-bearing and gold–silver stages of the Nezhdaninsk deposit and gold–rare metal ore mineralization of the Kurum massif vary, respectively, from +15.9 to +16.4‰, from +14.8 to +16.6‰, from +13.5 to +16.9‰, and from +10.3 to +12.6‰. The oxygen isotope composition of fluid was calculated as follows: +11.1‰ in equilibrium with metasomatites at 360°C, from +8.1 to +10.2‰ in equilibrium with quartz of the gold stage at 300°C (fluid I), from +5.2 to +8.6‰ in equilibrium with quartz of the gold–silver stage at 260°C (fluid II), and from +3.2 to +5.5‰ in equilibrium with quartz from rare metal mineralization at 290°C (fluid III) (Fig. 3). It is interesting that the fluids at the late stages were enriched in isotopically light oxygen. These data suggest that productive quartz precipitated from magmatic water (from +5.5 to +9.0‰).

The values of $\delta^{18}O$ in quartz from gold zones of the Maisk deposit vary from +11.8 to +14.5‰ (Bortnikov *et al.*, 2004). The quartz could crystallize from fluid with an oxygen isotope composition of $+6 \pm 2$‰ (fluid I) at 300°C (Fig. 3). This value is typical of magmatic fluid (Sheppard, 1986). The oxygen isotope composition of quartz from the wolframite-bearing veins formed at the cassiterite–sulfide stage varies from +6.4 to +16.1‰, which corresponds to $\delta^{18}O$ of water in the ore-forming fluid from –2.3 to +10.4‰ at 400°C (fluid II), indicating an increase in the variation of oxygen isotope ratios. The values of $\delta^{18}O$ in quartz from quartz–stibnite veins vary from +6.4 to +15.2‰. The oxygen isotope composition of water in the parent fluid varied from –5.1 to +3.5‰ at 200°C (fluid III). This indicates a contribution of heated meteoric waters in the formation of these veins. Thus, ores of the Maisk deposit precipitated from at least three different fluids (Fig. 3). The early gold-bearing veinlet-disseminated ores mainly precipitated from magmatogenic fluid; the gold–stibium ores, of supposedly epithermal origin, precipitated from heated meteoric waters; and quartz–cassiterite ores formed from a mixed magmatic–meteoric fluid.

At the Berezovsk deposit, hydrogen and oxygen isotope compositions were studied in the minerals of metamorphic rocks, wall-rock metasomatites, and quartz veins (Bortnikov *et al.*, 1997). The values of δD and $\delta^{18}O$ in minerals from metamorphic rocks (epidote, amphibole, chlorite, biotite, and serpentine) vary, respectively, from –48 to –87‰ and from +3 to +9.5‰. The values of δD and $\delta^{18}O$ in minerals from metasomatic rocks (sericite, fuchsite, and chlorite) vary from –48 to –63‰ and from +6.1 to +10.8‰. The values of δD and $\delta^{18}O_{H_2O}$ in equilibrium with metamorphic minerals at 350°C vary, respectively, from –12 to –34‰ and from +2.0 to +10.2‰, and those in equilibrium with metasomatic minerals at 275°C, from –39 to –63‰ and from +5.2 to +8.1‰, respectively. Such an isotope composition corresponds to the primary magmatic fluid (Fig. 4). The values of $\delta^{18}O$ in quartz from gold veins vary from +10.4 to +11.4‰ in early quartz and from +7.0 to +17.2‰ in late quartz, and those in quartz from sulfide–quartz veins of the Shartash massif, from +9.7 to +11.2‰. The oxygen isotope composition of the mineral-forming fluid in equilibrium with early quartz

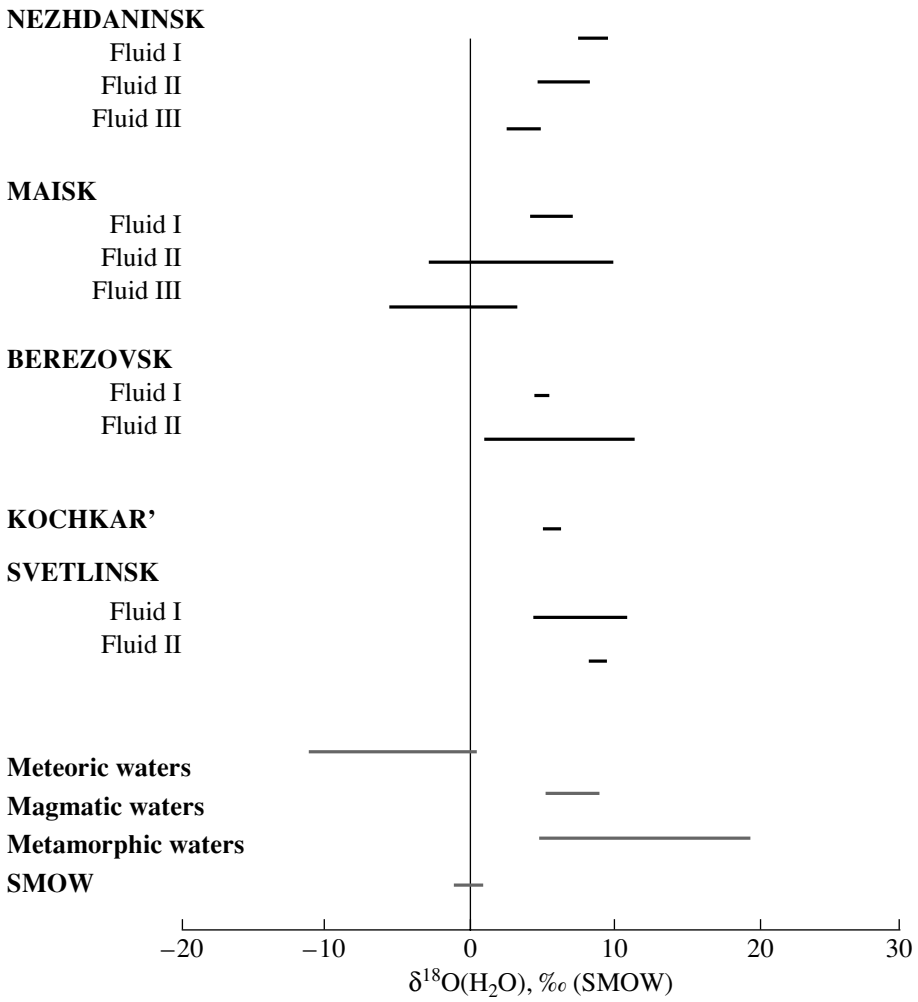

Fig. 3. Oxygen isotope compositions of the ore-forming fluid of the mesothermal gold deposits.

at 350°C varies from +4.8 to +5.8‰ (fluid I), and that in equilibrium with late quartz, from +1.4 to +11.6‰ (fluid II) (Fig. 3). Most data points fall in the magmatic water range (from +5.5 to +9.5‰ (Sheppard, 1986)). Metasomatic rocks and vein quartz formed from fluids with similar oxygen isotope compositions, suggesting a similar fluid source.

The values of $\delta^{18}O$ in quartz from sulfide–quartz veins in the northern block of the Kochkar deposit vary from +7.9 to +18.1‰. Most values are within the range from +12 to +14‰. The oxygen isotope composition of water in the fluid in equilibrium with quartz at 350°C is 5.8‰ (Fig. 3). This value is typical of magmatic water.

The values of $\delta^{18}O$ in quartz from the ore-bearing metasomatites of the Svetlinsk deposit vary from +15.9 to +16.4‰, and those in quartz from the quartz veins, from +6.9 to +7.5‰ and from +11.9 to +18.5‰ (Bortnikov *et al.*, 1999). The calculated $\delta^{18}O$ values at 300°C are as follows: 0 ± 1‰ and from +4.5 to +11.0‰ (fluid I) for the water in equilibrium with quartz of the gold-bearing veins, and from +8.5 to +9.0‰ (fluid II) for the water in equilibrium with quartz of the ore-bearing metasomatites (Fig. 3). Water that caused wall rock alteration was isotopically close to magmatic water (from +5 to +9.5‰). One group of the $\delta^{18}O_{H_2O}$ values in fluid that precipitated vein quartz (from +4.5 to +11.0‰) is typical of metamorphic and magmatic waters, while the other group is typical of meteoric waters or water formed during transformation of organic-rich rocks.

The data obtained indicate that gold-bearing fluids in the studied mesothermal systems consisted of a moderate- to low-salinity mixture of H_2O, CO_2, CH_4, N_2. Minerals began to precipitate owing to immiscibility of fluid into gas and liquid phases. At the subsequent stages, the mineral-forming system contained aqueous–salt fluid formed by fluid immiscibility and exsolution of the gas phase from the mineral-forming system. The oxygen isotope composition suggests that ores formed not only from magmatic fluids but also from fluids produced by metamorphism of the host rocks.

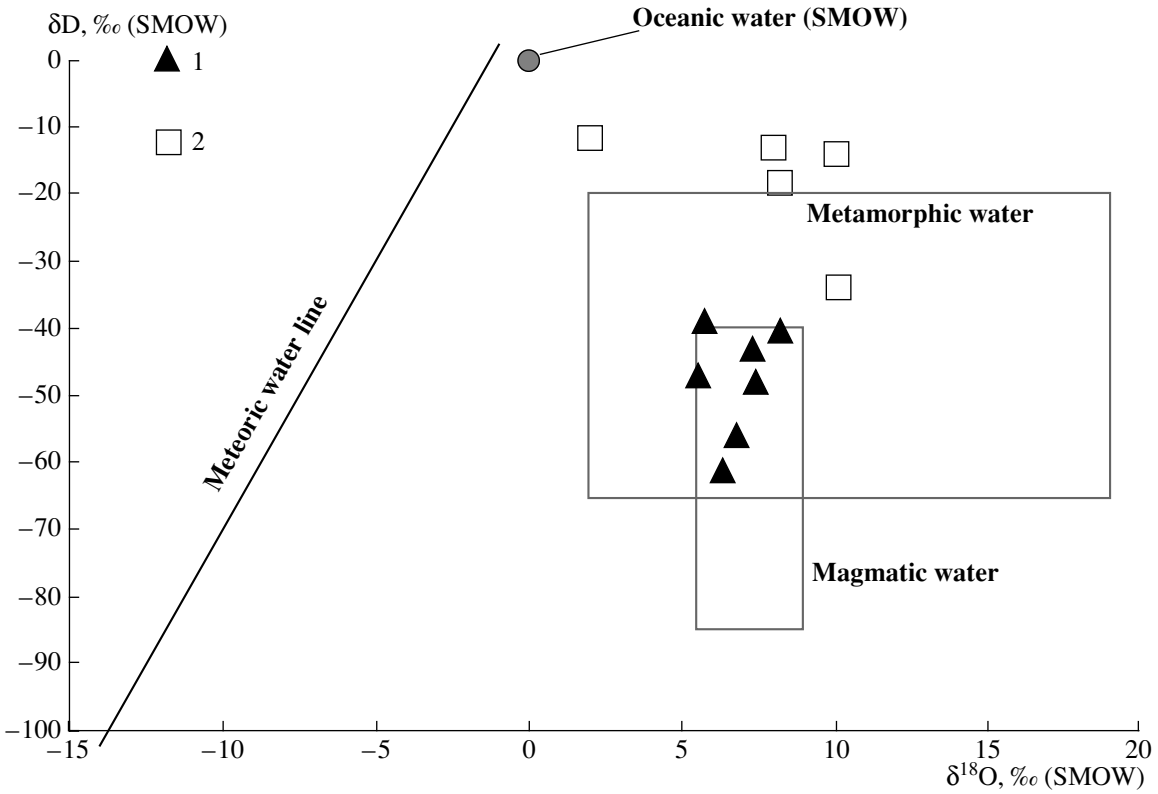

Fig. 4. Oxygen and hydrogen isotope compositions of fluid in equilibrium with minerals of the Berezovsk ore field. (1) Minerals of metasomatic rocks; (2) minerals of metamorphic rocks.

Thus, these investigations do not support the hypothesis that gold deposits of this type formed from only one (metamorphic, meteoric, or magmatic) fluid. This indicates a polygenic, magmatic–metamorphic origin of the ore-forming fluids. The variations in the chemical and isotope compositions of the mineral-forming fluid indicate that components were rapidly mixed at the ore precipitation site or near it (Bortnikov *et al.*, 1996). The magmatic fluid played a leading role. In my opinion, the most preferable genetic model of the formation of mesothermal gold deposits relates to the magmatic activity. In this case, fluid can be generated by different ways, including direct input from a magmatic chamber, mobilization of components during dehydration, decarbonatization during contact or contact–regional metamorphism, and involvement of deeply circulating meteoric waters (Bortnikov *et al.*, 1996, 1998, 1999, 2004).

CASSITERITE–SILICATE–SULFIDE DEPOSITS

Cassiterite–silicate–sulfide deposits are considered to be genetically or paragenetically related to granitoid magmatism. However, there is disagreement regarding the origin of mineral-forming fluids. Some geologists believe that tin-bearing fluids were exsolved from magma during crystallization, whereas others suggest that cassiterite deposits formed mainly from meteoric waters modified during heating and interaction with granitoids. Many tin ore systems bear evidence for involvement of both magmatic and meteoric waters in the mineral formation (Walshe, 1996).

We studied the geochemistry of ore-forming fluids at the Solnechnoe (Komsomol'sk tin district) and Arsen'evsk and Vysokogorsk deposits (Kavalerovo ore district) (Bortnikov *et al.*, 2005), which are localized in the Sikhote Alin accretionary fold system.

The Solnechnoe cassiterite–silicate deposit is confined to the intersection between the sublatitudinal Silinka and the sublongitudinal Solnechnoe faults, being hosted by Upper Jurassic quartz–feldspar sandstones, silty sandstones, and siltstones. It formed in two megastages: (1) an early molybdenum megastage, related to the monzogranite phase of the Silinka complex, and (2) a tin megastage, which produced quartz–tourmaline–cassiterite mineralized zones. Two tin megastages, early, Cretaceous, and late, Paleocene–Eocene, were identified at most tin deposits of the Kavalerovo district (Arsen'evsk, Dubrovsk, and Vysokogorsk).

Fluid Inclusions

Molybdenum megastage. Based on the phase composition at room temperature, three types of fluid inclusions were identified in quartz of different generations,

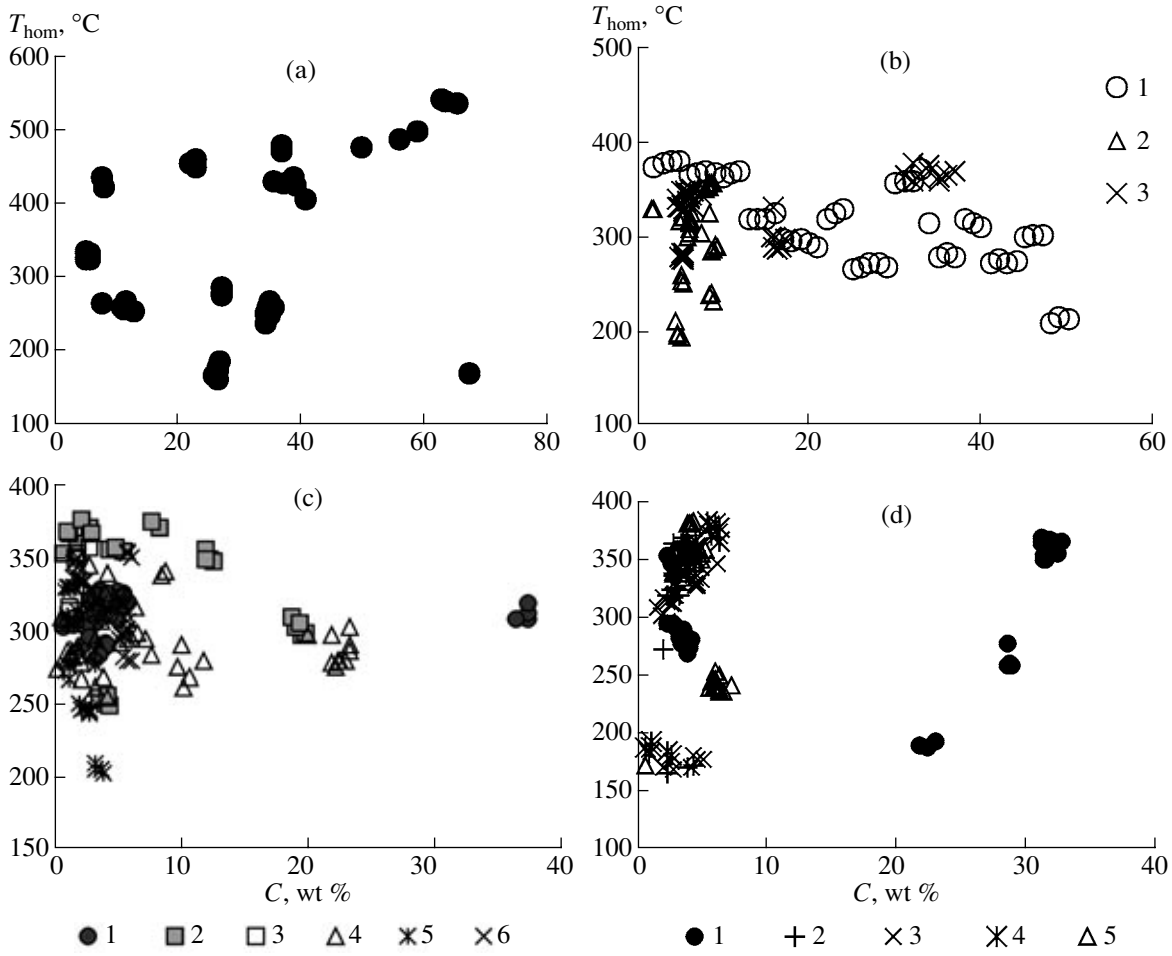

Fig. 5. Variations of homogenization temperature versus solution concentration of fluid inclusions in minerals of the molybdenum stage of the Solnechnoe deposit (a), in quartz of tin stage of the Solnechnoe deposit (b), in minerals of tin stage of the Vysokogorsk deposit (c), and in quartz of tin stage of the Arsen'evsk deposit (d). (a) (1) Quartz of different generations, tourmaline, fluorite, and apatite; (b) levels: (1) 522, (2) 582, and (3) 530 m; (c) (1) quartz, Glavnaya vein, (2) cassiterite, Northern vein, (3) quartz, Northern vein, (4) quartz, Aisk vein, (5) calcite, Ryabininsk zone, (6) quartz, Ryabininsk zone; (d) (1) Fel'zitovaya vein, (2–4) Southern vein, (5) Fevral'skaya vein.

tourmaline, fluorite, and apatite from the Solnechnoe deposit. Type I includes multiphase fluid inclusions found in quartz 1, fluorite, and apatite. They contain liquid (solution), a vapor bubble, and one to three or more crystals (halite, sylvite, possibly $CaCl_2 \cdot 6H_2O$, and $MgCl_2$ hydrate). Type II comprises two-phase (liquid + vapor) fluid inclusions found in quartz 2, fluorite, tourmaline, and quartz 3. Type III includes single-phase vapor inclusions in quartz 1 (Bortnikov *et al.*, 2005). Fluid inclusions of types I and III occur in the same growth zones in quartz I, indicating almost simultaneous entrapment.

Hence, minerals precipitated from fluids of different phase and chemical composition. The presence of syngenetic aqueous–salt and gas inclusions homogenizing at 480°C indicates that minerals crystallized due to phase separation into liquid aqueous–salt and aqueous–vapor fluids. At lower temperatures, minerals of the molybdenum megastage precipitated from a homogeneous aqueous–salt fluid. The mineral-forming system contained high-salinity fluids with a predominance of Na, Ca, and Mg chlorides, as well as fluids with moderate and low contents of mainly Na (and Mg) chloride. The fluid composition varied with decreasing temperature (Fig. 5a): high-temperature (>480°C) aqueous–salt fluid with extremely high salinity (brine–melt?) from 65 to 50 wt % NaCl equiv with decreasing temperature (440–410°C) evolved through a high-salinity brine (40–20 wt % NaCl equiv) to a moderate-salinity and dilute fluid with salinity 5–15 wt % NaCl equiv. However, when the temperature decreased below 300°C, the fluid salinity again increased up to 35–25 wt % NaCl equiv. The fluid, in addition to predominant water, contained NH_4, N_2, and occasional CO_2.

Tin megastage. Three types of inclusions were distinguished on the basis of the phase composition at room temperature. Type I consists of solution, a vapor bubble, and one or several crystals: halite and one or

several anisotropic crystals. Type II comprises two-phase fluid inclusions consisting of solution and a vapor bubble. Type III consists of single-phase vapor-rich fluid inclusions.

Cassiterite–silicate–sulfide veins were deposited from at least three chloride (chloride–bicarbonate) aqueous–salt fluids, which differed in cationic composition and contents of dissolved salts. They contained 99.3–98.9 mol % H_2O and a total of 1 mol % CO_2, CO, CH_4, and N_2. The vapor composition of the fluids varied from mostly CH_4 to CO_2. Fluids of mainly Na chloride or Na chloride–bicarbonate composition played the main role in the tin ore formation. The salinity of Na chloride (Na chloride–bicarbonate) fluids varied from moderate to low (16–0.7 wt % NaCl equiv). In addition, the observation of vapor inclusions syngenetic to aqueous–salt fluid inclusions indicates the fluid separation in the mineral-forming environment.

The studied samples from the Solnechnoe and Arsen'evsk deposits contain high-density (1.13–1.10 g/cm^3) brines with salinity 34.9–30.1 wt % NaCl equiv, while fluid inclusions in cassiterite and quartz from the Vysokogorsk deposit contain lower salinity (23.1–2.6 wt % NaCl equiv) (Figs. 5b, 5d) and dense (0.97–0.59 g/cm^3) brines (Fig. 5c). These fluids typically show the highest temperatures: fluid inclusions in minerals from the Solnechnoe and Arsen'evsk deposits homogenized at 378–350°C, and those in minerals from the Vysokogorsk deposit, at 377–276°C. They sharply differ from inclusions trapped in tin-megastage minerals but are similar to inclusions trapped in the molybdenum-megastage minerals of the Solnechnoe deposit.

Fluid inclusions in quartz and cassiterite of typical veins of the Vysokogorsk deposit and in the Fel'zitovaya vein of the Arsen'evsk deposit contain Ca–Na chloride solutions with high salinity (40.0–18.5 wt % NaCl equiv) and density (1.15–0.91 g/cm^3). These fluids are of lower temperature, with homogenization temperatures below 320°C.

Thus, the molybdenum mineralization and tin ores at the studied deposits precipitated under different *PT* conditions and from chemically different fluids. The molybdenum mineralization formed at higher temperatures (up to 540°C) from extremely saline (65–60 wt % NaCl equiv) to high- (30–20 wt % NaCl equiv) and moderate-salinity (15–5 wt % NaCl equiv) fluids dominated by Mg and Ca chlorides at 3–0.4 kbar. The cassiterite–quartz veins crystallized at lower temperatures from 390 to 190°C and pressures below 0.3 kbar, mainly from low-salinity fluids dominated by Na chloride. However, the tin-forming solutions were chemically different. The cassiterite–quartz veins formed in a transform margin setting (the Solnechnoe and Vysokogorsk deposits and the Fel'zitovaya vein at the Arsen'evsk deposit) also precipitated from fluids containing Mg and Ca chlorides, whereas the cassiterite–quartz veins of the main vein system at the Arsen'evsk deposit were formed from Na–Cl fluid.

Oxygen Isotope Composition

The oxygen isotope composition was studied in quartz, cassiterite, and chlorite. Minerals from the Arsen'evsk deposit show the following variations in oxygen isotope composition: from +4.8 to +13.9‰ in quartz, from +0.1 to +5‰ in cassiterite, and from –1.5 to +2‰ in chlorite. At the Solnechnoe deposit, oxygen isotope compositions are from +8.7 to +12‰ in quartz, from +1.9 to +2.6‰ in cassiterite, and +4.2‰ in chlorite.

It was found (Bortnikov *et al.*, 2005) that the $\delta^{18}O$ values of the water in equilibrium with precipitating quartz, cassiterite, chlorite, and biotite in the ores of the Solnechnoe deposit are from +3.0 to +7.9‰, from +5.9 to +6.6‰, and +5.8‰, respectively, while those in the water in equilibrium with quartz and cassiterite at the Vysokogorsk deposit are from +5.3 to +8.7 and from +7.8 to +9.5‰, respectively. The $\delta^{18}O$ values in the water in equilibrium with quartz, cassiterite, and chlorite at the Arsen'evsk deposit vary from –1.3 to +8.3‰, from +3.9 to +9‰, and from –0.9 to +3.6‰, respectively (Fig. 6a). Such variations can be caused by mixing of fluids with different oxygen isotope composition. The mixing should be rapid and occur at the site of mineral precipitation to prevent isotope homogenization of the fluids.

Most of the $\delta^{18}O_{H_2O}$ values in the fluid that formed cassiterite–sulfide veins of the Solnechnoe, Vysokogorsk, and Arsen'evsk deposits fall in the magmatic water field ($\delta^{18}O$ ~ 5–9.5‰). However, the ore formation presumably involved fluids of different origin. The $\delta^{18}O_{H_2O}$ values of the tin ore zone of the Solnechnoe deposit are lower than the typical values of magmatic waters. Some shift toward lower values can be explained by mixing with a subordinate amount of isotopically light meteoric water. Cassiterite–quartz–chlorite veins of the Arsen'evsk deposit precipitated from fluids enriched in isotopically light oxygen. The low $\delta^{18}O$ values suggest a contribution of heated seawater ($\delta^{18}O$ ~ 0‰) or meteoric waters. However, the participation of seawater seems to be highly improbable. Hence, tin ores of the Arsen'evsk deposit formed by mixing between magmatic and meteoric waters.

Hydrogen and Oxygen Isotope Compositions

The hydrogen and oxygen isotope compositions were studied in the hydrous minerals tourmaline and biotite from the Solnechnoe deposit and tourmaline from the Vysokogorsk deposit. The obtained δD and $\delta^{18}O$ values were, respectively, as follows: from –103.6 to –101.1‰ and from +9.1 to +10.1‰ and –128.3 and +6.4‰ in tourmaline and biotite from the Solnechnoe deposit, and –154.2 to –135.2‰ and +10.3 to +12.9‰ in tourmaline from the Vysokogorsk deposit. The δD and $\delta^{18}O$ values of fluid in equilibrium with tourmaline and biotite, vary from –99.5 to –80.5‰ and from +7.5 to +10.1‰ at the Vysokogorsk deposit and from –102

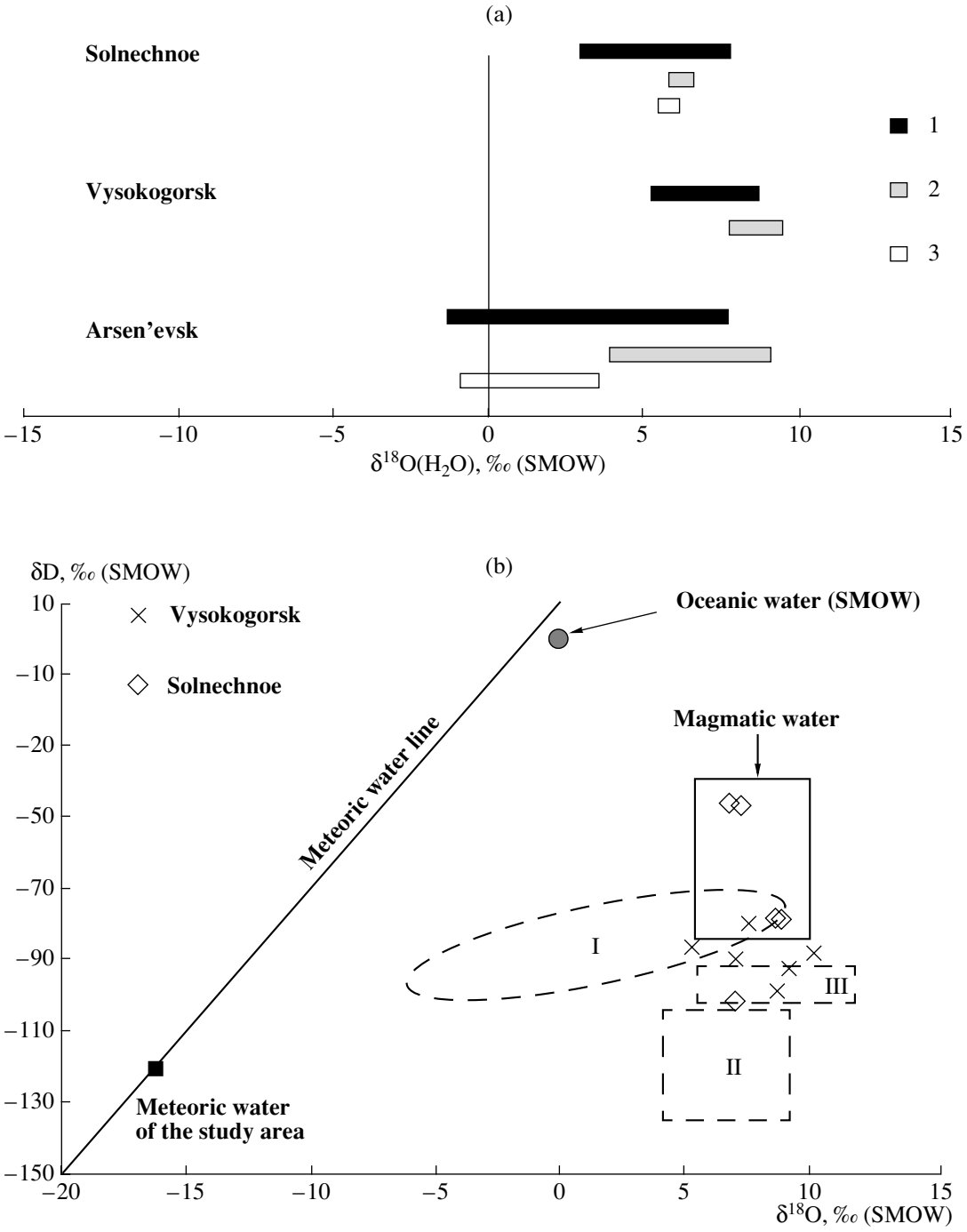

Fig. 6. Oxygen and hydrogen isotope compositions of fluids from different tin deposits. (a) Oxygen isotope composition of fluid in equilibrium with quartz (1), cassiterite (2), and chlorite (3) from the Solnechnoe, Vysokogorsk, and Arsen'evsk deposits; (b) tin deposits associated with the Mole Granite (I) (Heinrich, 1995), Iultin (II) (Spasennykh, 2002), Spokoininsk (III) (Matveeva, 2002), and Solnechnoe and Vysokogorsk deposits (original data).

to –46.4‰ and from +6.8 to +8.9‰ at the Solnechnoe deposit, respectively. These data indicate that the hydrogen and oxygen isotope compositions of the mineral-forming fluid at the Solnechnoe deposit fall in the field of magmatic water (Fig. 6b). The mineral-forming fluid of the Vysokogorsk deposit shows some D depletion relative to magmatic waters. Magmatic fluids can have a lower δD. This phenomenon is related to the magma degassing with exsolution of high-D fluid. This process causes a decrease in δD in the residual melt (Taylor, 1986; Hedenquist *et al.*, 1998). Magmatic bodies emplaced at the upper crustal levels interact with

meteoric waters, thus causing a change in hydrogen rather than oxygen isotope composition (Taylor, 1986). Therefore, water exsolved from such contaminated magma during crystallization can differ in a lower δD relative to the primary magmatic water. Meteoric waters played a lesser role in the deposition of studied cassiterite–sulfide deposits as compared to similar deposits from other regions (Fig. 6b).

Thus, the study of oxygen and hydrogen isotope compositions indicates a leading role of magmatic fluid during formation of the tin deposits, with involvement of heated meteoric waters.

Sulfur Isotope Composition

The sulfur isotope composition varies from –2.5 to –0.4‰ in molybdenite from the Solnechnoe deposit, from –4.2 to +6.7‰ in galena from the Arsen'evsk deposit, and from –3.3 to –2.3‰ in galena from the Vysokogorsk deposit. The $\delta^{34}S$ values in sphalerite vary from –3.5 to +2.1‰ at the Arsen'evsk deposit and from –1.5 to +0.9‰ at the Vysokogorsk deposit. These data indicate that the minerals formed from fluid with $\delta^{34}S_{H_2S}$ from –4 to +2‰. According to modern concepts, $\delta^{34}S$ in mantle sulfur varies from –3 to +2‰. The $\delta^{34}S_{H_2S}$ values in magmatic fluids associated with *S*-type granites are between –3 and +5‰. This indicates a significant contribution of "mantle" sulfur in the ores. Fluids that formed molybdenite at the Solnechnoe deposit and galena and sphalerite at the Vysokogorsk and Arsen'evsk deposits fall in the same field.

The obtained chemical and isotope data on fluids made it possible to determine their origin. Minerals from ore deposits contain inclusions with high-temperature (>500°C) and high-salinity (>40 wt % NaCl equiv) fluids, which occasionally coexist with melt inclusions. It was proposed that brines formed by exsolution from silicate melt (Candela and Piccoli, 1995; Shinohara, 1994). This hypothesis was later supported by experimental data and study of fluid and melt inclusions, which showed that silicate melt with moderate Cl content can coexist with both liquid and vapor under melt–fluid unmixing conditions (Lowenstern, 1995). The study of melt and fluid inclusions in the minerals of deposits associated with the Mole Granite, Australia, and simulation of the melt and fluid evolution (Audetat *et al.*, 2000) showed that two fluids exsolved from microgranite melt at the late stage: brines with salinity 37–40 wt % NaCl equiv and vapor-rich fluid with salinity 4 wt % NaCl equiv. Such a scenario can be applied to the evolution of the ore-magmatic system at the Solnechnoe deposit.

These data indicate that tin ores of the studied deposits formed by mixing of at least three fluids at the sites of mineral deposition: high-density brines and low-salinity vapor-rich fluid exsolved from granite magma during crystallization and fluid of meteoric origin. The high-density highly saline brine and low-density low-saline vapor-rich fluid were exsolved during crystallization of granite melt. Less saline brines were accumulated at the deep levels of the ore-forming system. Under hydrostatic pressure, rapidly ascending vapor-rich fluid could form a plume (Henley and McNabb, 1978), which entrapped brine, thus decreasing the total salinity of the fluid. Hence, mixing of two fluids and dilution of the brines probably occurred at the deep levels of the mineral-forming system. Under near-surface conditions, the magmatic fluid produced interacted with meteoric waters, causing subsequent dilution.

VEIN SILVER–BASE METAL DEPOSITS

Silver–base metal deposits of the Verkhoyansk region are spatially associated with tin deposits, which are genetically related to granitoid magmatism. The silver–base metal deposits are most distal from intrusions, being zonally distributed around them (Nekrasov, 1963; Flerov, 1984). It is believed that these deposits were generated by the ore-magmatic systems triggered by the emplacement of granitoids at the final stages of late-collisional processes. These systems were initiated during collision of the Kolyma–Omolon terrane with the Siberian continent. These systems were related to vertical extensional faults, which were formed in a compressional setting and oriented normal to the converging continental blocks (Parfenov, 1995). The systems produced polychronous deposits. Silver–sulfide–tin ores formed at the early stage, and silver–base metal ores, at the late stage. The silver–sulfide–tin mineralization is made up of lenslike veins, stockworks, vein systems, and mineralized zones among granitoids and hornfelses. The silver–base metal ores compose mineralized and vein–disseminated zones among subvolcanic granodiorite- and granite-porphyries and terrigenous sequences of the Verkhoyansk complex, which experienced wall rock silicification.

The mineral–geochemical evolution of the silver–sulfide–tin ores involves subsequent spatial and temporal replacement of iron-free silicates and oxides by ferruginous oxides, sulfoarsenides by sulfides and then carbonates, and tin oxides by tin sulfides (stannite) and tin sulfosalts (franckeite, hocartite). The silver–base metal ores demonstrate subsequent replacement of sulfide–carbonate mineral aggregates by quartz–sulfide–sulfosalt assemblages and again by essentially carbonate minerals. Carbonates are siderite (coarse-grained and rhythmically zoned), zoned ankerite and dolomite, and latest calcite. These ores are abundant in fahlore with moderate to high Ag content (20–50 wt %) and silver sulfosalts (owyheeite, andorite, ramdohrite, diaphorite, pyrargyrite, and myrargyrite).

This raises the question whether magmatic chambers associated with silver–base metal deposits were only heat sources, which induced a convective cell, or produced fluid, which transferred metals and ligands?

To solve this question, fluid inclusions and the stable isotope composition (C, O, S) in minerals were studied at the Prognoz silver–base metal deposit, formed in two stages (Gamyanin *et al.*, 1998, 2003; Anikina *et al.*, 1999), and the Kupol'noe tin–silver–base metal deposit, formed in three stages (rare metal, tin–silver–base metal, and silver–stibium) (Gamyanin *et al.*, 2001).

Fluid Inclusions

Characteristics of fluid inclusions. Primary fluid inclusions 5–20 μm in size of negative crystal or irregular shape were found in carbonate and quartz of three generations at the Prognoz deposit. They consist of two phases at room temperature: (1) liquid, supposedly, water with dissolved salts and (2) vapor, mostly CO_2.

Minerals from the Kupol'noe deposit contain primary and secondary fluid inclusions 15–5 μm in size, which in phase composition at room temperature are subdivided into three types. Type I includes two-phase vapor-rich inclusions. Type II involves two-phase inclusions consisting of liquid and a vapor bubble. Type III is three-phase inclusions consisting of a solid phase represented by halite or a xenogenic tabular or platy solid phase (>5 μm), as well as liquid and vapor. The secondary fluid inclusions were mainly found in quartz I and quartz II. Simultaneous entrapment of fluid inclusions with variable liquid/vapor ratios presumably indicates vapor separation from the mineral-forming fluid (Roedder, 1984). Fluid inclusions of types I and III were found in the same growth zones of quartz, indicating their simultaneous formation. This can be used as evidence for crystallization of quartz I from "boiling" fluid (Bodnar *et al.*, 1984).

Microthermometric measurements. In the Prognoz deposit, the homogenization temperatures of fluid inclusions range within 185–155°C for quartz I, within 215–145°C for quartz II, and within 195–120°C for quartz III. Fluid inclusions in carbonates homogenized at lower temperatures: 155–145°C in siderite I, 185–180°C in siderite II, and 110–100°C in Fe-calcite. It was found that aqueous solutions trapped by fluid inclusions contained dissolved NaCl and $CaCl_2$ and significant amounts of dissolved KCl and $FeCl_2$ (Gamyanin *et al.*, 1998). The salinity of the trapped solution varies from 29.0 to 8.0 wt % NaCl equiv. The vapor phase consists of CO_2 (65.4–94.2%), N_2 (5.0–29.5%), and CH_4 (0.8–5.1%).

Fluid inclusions in minerals from the Kupol'noe deposit homogenized at 450–125°C, indicating that this deposit formed within a significantly higher temperature range than the Prognoz deposit. Fluid inclusions in the early quartz homogenized at the highest temperatures (285–450°C), while fluid inclusions in quartz III and IV homogenized at lower temperatures (210–125 and 280–135°C).

Type 3 fluid inclusions contain high-salinity chloride solutions with 36–38 wt % $CaCl_2$ + NaCl, while fluid inclusions of types 1 and 2 have salinity 10.5–3.3 wt % NaCl equiv and contain NaCl and $FeCl_2$. Fluid inclusions in quartz III, in addition to NaCl, contain $FeCl_2$ and $CaCl_2$ with salinity 9.2–3.3 and 7.9–3.3 wt % NaCl equiv, respectively.

Stable Isotopes

Oxygen isotope composition. In the Prognoz deposit, oxygen isotope composition was studied in quartz from metasomatic veinlets (quartz II), as well as in veined fine-grained (quartz IIIa) and druse (quartz IIIb) quartz. The $\delta^{18}O$ value was +14.7 ± 0.4‰ in quartz II, +9.3 to +12.5‰ in quartz IIIa, and +11.1 ± 0.4‰ in quartz IIIb (Fig. 7a). The $\delta^{18}O_{H_2O}$ value in the metasomatic fluid in equilibrium with quartz at 200°C was approximately +3.1 ± 1‰. The $\delta^{18}O_{H_2O}$ value of fluid in equilibrium with veined fine-grained quartz varied from –2.3 to +0.9‰, while, for fluid in equilibrium with microdruse quartz, it was –0.4 ± 1‰.

The $\delta^{18}O_{H_2O}$ values of fluid in equilibrium with ankerite at 150–200°C fall in two intervals: from –4.6 to –1.6‰ and from +7.4 to +16.1‰. The oxygen isotope composition of fluid in equilibrium with carbonates indicates that fluids from two isotopically different sources contributed to the mineral-forming system at late stages: one source with isotopically light meteoric water ($\delta^{18}O_{H_2O}$ approximately from –4 to –1‰) and one with isotopically heavy water ($\delta^{18}O_{H_2O}$ approximately from +7 to +16‰). The isotopically heavy water could have been of magmatic–metamorphic origin or the fluid in equilibrium with metamorphic waters. Variations in the oxygen isotope composition are explained by mixing of these fluids in different proportions and boiling.

The $\delta^{18}O$ values in quartz of different generations from the Kupol'noe deposit are as follows: from +6.2 to +7.9‰ in quartz I, from +7.1 to +8.9‰ in quartz II, from +2.3 to +5.5‰ in quartz III, and from +8.3 to +11‰ in quartz IV (Fig. 7a). It should be noted that the oxygen isotope compositions in quartz of each generation vary in narrow ranges and differ from each other: the highest $\delta^{18}O$ values are typical of quartz IV, while the lowest values are observed in quartz III. The oxygen isotope composition of water, the main component of hydrothermal fluid, was calculated in the quartz–water system at 350°C for quartz I and II. The obtained $\delta^{18}O_{H_2O}$ value was +4 ± 2‰. The exsolution of CO_2 with a temperature and pressure drop causes a decrease in $\delta^{18}O$ of residual fluid (Bowers, 1991). Evidently, fluid was higher in heavy oxygen before stratification. The $\delta^{18}O_{H_2O}$ value of fluid in equilibrium with quartz III

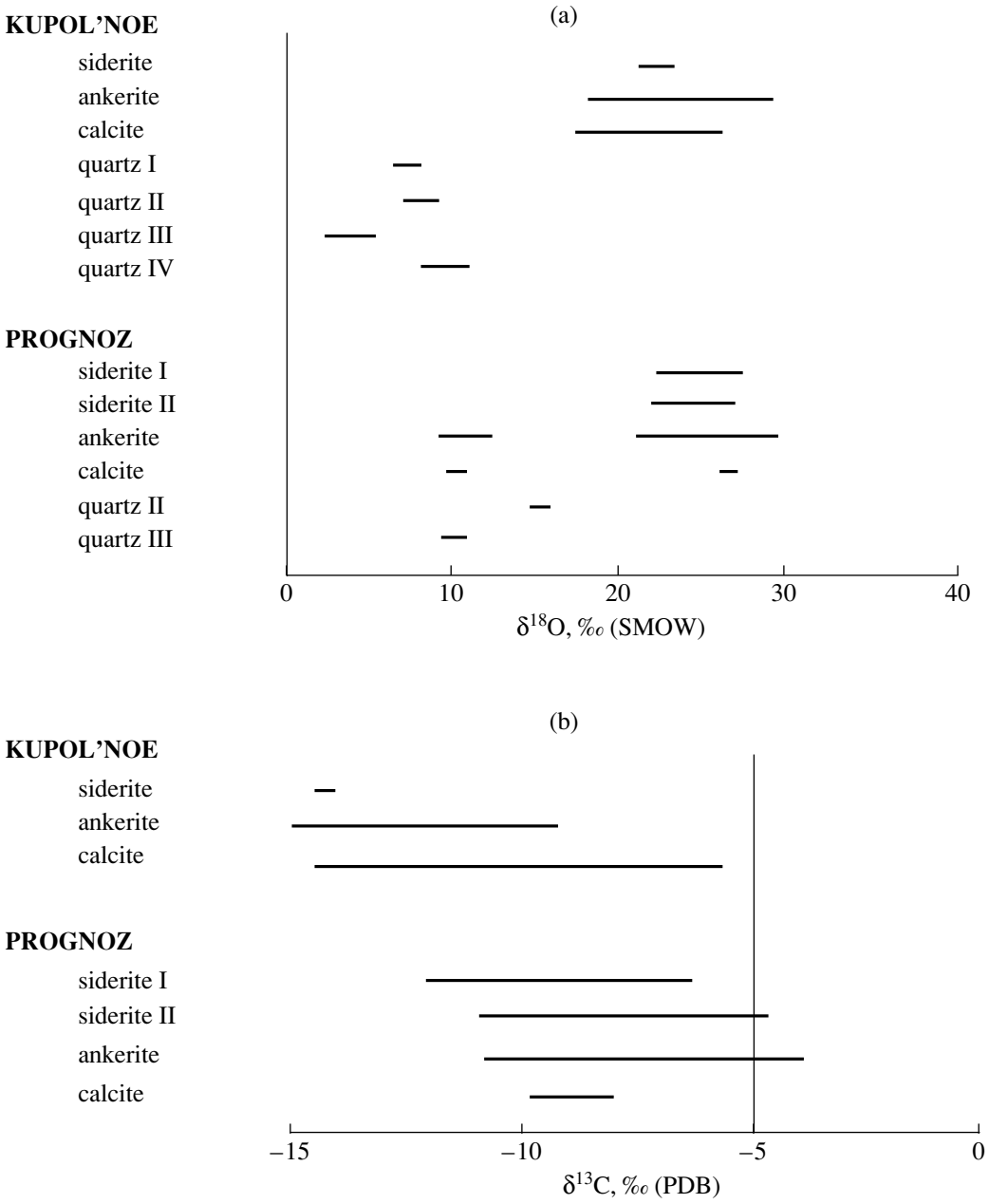

Fig. 7. Oxygen (a) and carbon (b) isotope compositions of minerals from the vein silver–base metal deposits.

at 200°C was –8 ± 3‰. The calculated $\delta^{18}O_{H_2O}$ value of fluid in equilibrium with quartz IV at 275°C is +2 ± 2‰.

Carbon and oxygen isotope compositions of carbonates. The $\delta^{13}C$ values in carbonates of different ages from the Prognoz deposit show no significant differences, falling mostly within a narrow range from –9 to –7‰. These data indicate no significant evolution in the carbon isotope composition of carbonates. The oxygen isotopes behave in a different manner: $\delta^{18}O$ values in early carbonates (siderite 1 and 2) fall in a narrow range from +24 to +28‰, demonstrating wider variations from +9.1 to +29.8‰ and from +9.6 to +27‰ in late carbonates (ankerite and calcite, respectively) (Fig. 7b).

The carbon and oxygen isotope compositions in carbonates of the two early generations at the Prognoz deposit fall in a single field, while the two late generations are clustered into two groups with different oxygen isotope composition at close $\delta^{13}C$ values. Hence, no correlation is observed between carbon and oxygen isotope compositions.

Different carbonates from the Kupol'noe deposit mostly have similar $\delta^{13}C$ values, around –14.4 ± 3‰, with only two exceptions (–9.2 and –5.6‰). Hence,

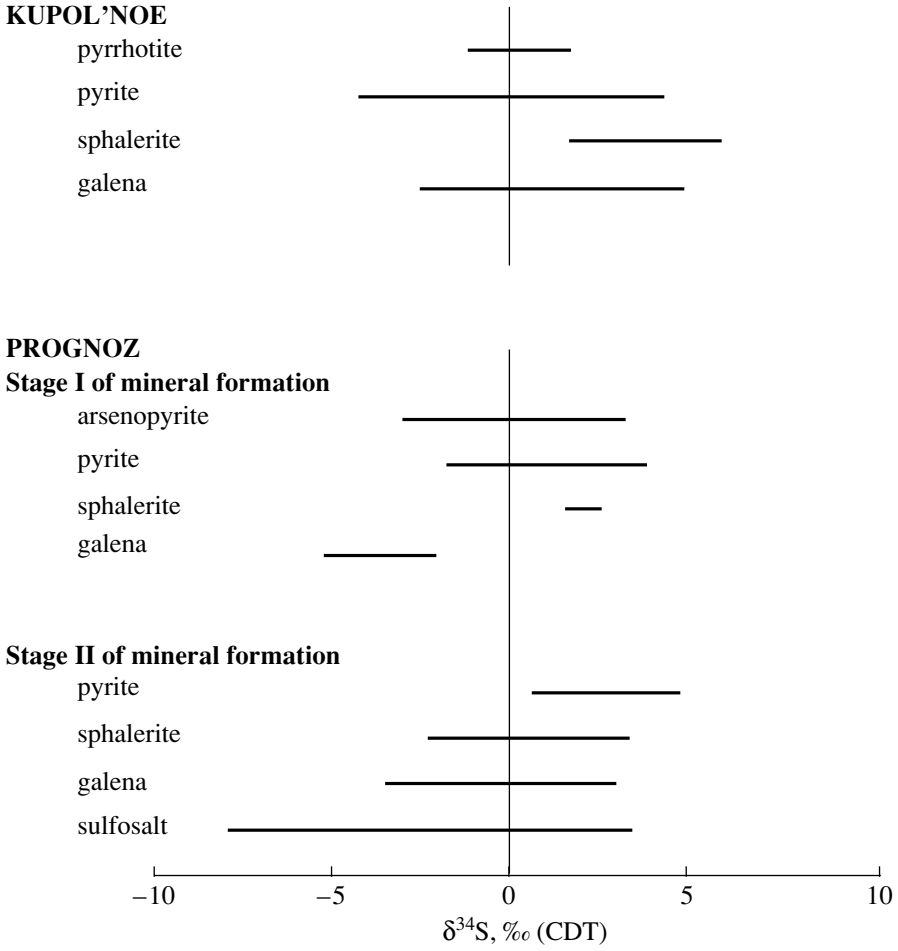

Fig. 8. Sulfur isotope composition in sulfides and sulfosalts of vein silver–base metal deposits.

carbon isotope compositions in carbonates experienced no significant evolution. The carbon isotope composition in hydrothermal fluid was calculated for dissolved CO_2 at 140–185°C. The $\delta^{13}C_{CO_2}$ value of fluid in equilibrium with siderite was –20 ± 1‰. These values could vary from –17.6 to –10.2‰ for fluid in equilibrium with ankerite and were equal to –14.5 for fluid in equilibrium with calcite.

The $\delta^{18}O$ values in carbonates vary between +17.4 and +29.2‰: from +21.4 to +23.5‰ in siderite, from +18.2 to +29.2‰ in ankerite, and from +17.4 to +26.4‰ in calcite (Fig. 7a). The widest variations are typical of oxygen isotope compositions of ankerite. The values of $\delta^{18}O$ in other minerals are grouped in a narrow range.

Sulfur isotope composition of sulfides. The study of the sulfur isotope composition in sulfides of different age and sulfosalts from the host rocks, metasomatic rocks, and different associations from the orebodies of the Prognoz deposit showed significant variations in $\delta^{34}S$ (Fig. 8), though most values (more than 70%) fall between –2 and +3‰. Later minerals show narrower variations of $\delta^{34}S$ values.

The $\delta^{34}S_{H_2S}$ values of fluid in equilibrium with the first-stage sulfides on a temperature decrease from 300 to 180°C were calculated to vary from –3.7 to +2.7‰. The $\delta^{34}S_{H_2S}$ values of the mineral-forming fluid in equilibrium with different minerals of the second stage varied significantly (from –2.9 to +6.5‰), with the isotopically heaviest sulfur signatures found for fluid in equilibrium with late sulfide, galena.

The $\delta^{34}S$ value in sulfides from the Kupol'noe deposit vary from –4.2 to +6‰ (Fig. 8). The $\delta^{34}S_{H_2S}$ value in the early fluid in equilibrium with pyrite 1 is within 0 ± 3‰. The sulfur isotope composition of fluid at 185–125°C varies from +0.6 to +8.9‰ in equilibrium with galena and from +1.2 to +5.5‰ in equilibrium with sphalerite. The $\delta^{34}S_{H_2S}$ value in fluid could be close to ~+3 ± 2‰. The sulfur isotope composition of fluid in equilibrium with silver–stibium mineralization was calculated from $\delta^{34}S$ obtained for pyrite from this assemblage. The obtained $\delta^{34}S_{H_2S}$ value of fluid in equilibrium with pyrite is –1 ± 2‰.

Evidently, the Prognoz and Kupol'noe deposits formed under sharply different fluid regimes. Different mineral aggregates in veins of the Prognoz deposit, which were separated by emplacement of quartz porphyry and granite porphyry dikes between 113 and 82 Ma, formed under similar physicochemical conditions at relatively low temperatures (250–100°C) from reduced H_2O–CH_4–N_2–CO_2 moderate-salinity (8.0–29.0 wt % NaCl + $CaCl_2$) chloride solutions. In spite of the variations in temperature and contents of salts and dissolved gases, the fluids experienced no significant changes during ore precipitation. The sulfur and carbon isotope compositions in minerals of different stages also showed no significant changes. These data indicate that the deposit formed during long evolution of an ore-forming hydrothermal system related to the same reservoirs. Fluid with a carbon isotope composition from –3 to –5‰ contained deeply sourced carbon related to granitoid magmatism with an accepted $\delta^{13}C_{CO_2}$ value from –3 to –5‰ (Ohmoto, 1986). Fluid that precipitated early-stage mineral aggregates was enriched in isotopically heavy oxygen, indicating an important role of magmatic–metamorphic waters in the mineral-forming fluid. At the late stages, fluid was introduced from two sources having different oxygen isotope compositions: isotopically light meteoric water ($\delta^{18}O_{H_2O}$ approximately from –4 to –1‰) and isotopically heavy presumably magmatic–metamorphic water ($\delta^{18}O_{H_2O}$ from ~+7 to +16‰). The study of fluid inclusions suggests that high-salinity fluid (>30 wt % NaCl + KCl) was diluted by low-salinity fluid at the site of ore precipitation. Hence, the Prognoz deposit originated from fluids that were supplied from different sources: low-salinity meteoric waters and high-salinity magmatic hydrothermal solutions, which extracted sulfur and carbon from host rocks. Variations of chemical and isotope compositions in the mineral-forming fluid indicate rapid mixing of the components within or near the precipitation site.

By contrast, ores of the Kupol'noe deposit were derived from chemically and isotopically contrasting fluids. Rare metal mineralization precipitated from high-salinity (36–38 wt % NaCl equiv) aqueous brine, which coexisted with vapor-rich dilute aqueous low-salinity fluid (4.9–3.3 wt % NaCl equiv). The $\delta^{18}O$ values of +4 ± 2‰ probably indicate the contribution of magmatic waters ($\delta^{18}O$ from +5 to +9.5‰). The sulfur isotope composition in fluid generating rare metal ores is 0 ± 3‰, which corresponds to $\delta^{34}S$ values typical of mantle or magmatic origin (Ohmoto, 1986). Hence, the rare metal mineralization precipitated from granite-related fluid.

Tin–silver–base metal mineralization formed from low- to moderate-salinity fluid (9.2–3.3 wt % NaCl equiv). The oxygen isotope composition of this fluid ($\delta^{18}O = -8 \pm 2$‰) indicates a significant contribution of heated meteoric waters. ^{13}C-depleted ($\delta^{13}C$ from –14 to –20‰) fluid presumably indicates participation of organic carbon ($\delta^{13}C$ up to –30‰; Field and Fifarek, 1985) in the ore formation. The sulfur isotope composition ($\delta^{34}S_{H_2S} = -1 \pm 2$‰) of the fluid is typical of magmatic or mantle sulfur. Hence, fluid that precipitated tin–silver–base metal ores consisted of heated altered meteoric waters, which contained CH_4 and CO_2 extracted from the host magmatic and sedimentary rocks. H_2S was probably also taken from the host magmatic rocks.

Silver–stibium ores precipitated from dilute fluids with salinity 7.9–3.3 wt % NaCl equiv. The oxygen isotope composition of this fluid ($\delta^{18}O = +2 \pm 2$‰) presumably indicates a significant contribution of heated meteoric waters, while the sulfur isotope composition ($\delta^{34}S_{H_2S} = +3 \pm 2$‰) suggests its magmatic origin.

Ores of the Prognoz deposit presumably precipitated owing to activity of a long-term ore-forming hydrothermal system sourced from the same reservoirs, whereas the Kupol'noe deposit resulted from juxtaposition of ores generated by different hydrothermal–magmatic systems.

EPITHERMAL DEPOSITS

Epithermal deposits include nonferrous and precious metal deposits formed under relatively low temperatures (<300°C) in near-surface conditions (roughly at depths of 1–2 km). The term "epithermal deposits" was introduced by Lindgren. These deposits are typically divided into two groups (Hayba *et al.*, 1985). The first group is characterized by the high oxidation state of sulfur during ore formation ("high-sulfidation epithermal ore deposits") and abundant alunite among metasomatically altered rocks. The second group includes deposits formed under relatively reducing conditions ("low-sulfidation epithermal ore deposits"), with orebodies associated with adularia-bearing quartz–sericite metasomatic rocks. According to the generally accepted hypothesis, "low-sulfidation" epithermal ores formed from heated low-salinity meteoric waters, while magmatic fluid significantly contributed to "high-sulfidation" epithermal ores (Hedenquist and Lowenstern, 1994).

The composition and origin of the fluid in epithermal ore-forming systems can be illustrated by Ag–Bi–Pb–Zn deposits of the Adrasman–Kanimansur ore field, located in the Karamazar ore district. With respect to mineral composition, two types of ores can be distinguished there: copper–bismuth and silver–lead. The copper–bismuth ores are localized at the deeper levels of deposits, and silver–lead ores, at the higher levels (Safonov *et al.*, 2000a, 2000b). Quartz–hematite–chlorite and quartz–chalcopyrite–pyrite veinlets and veins formed at the early stage. Fluorite–sulfide veinlike bodies, galena–sphalerite–barite veins, and vein–disseminated mineralization formed at the second stage.

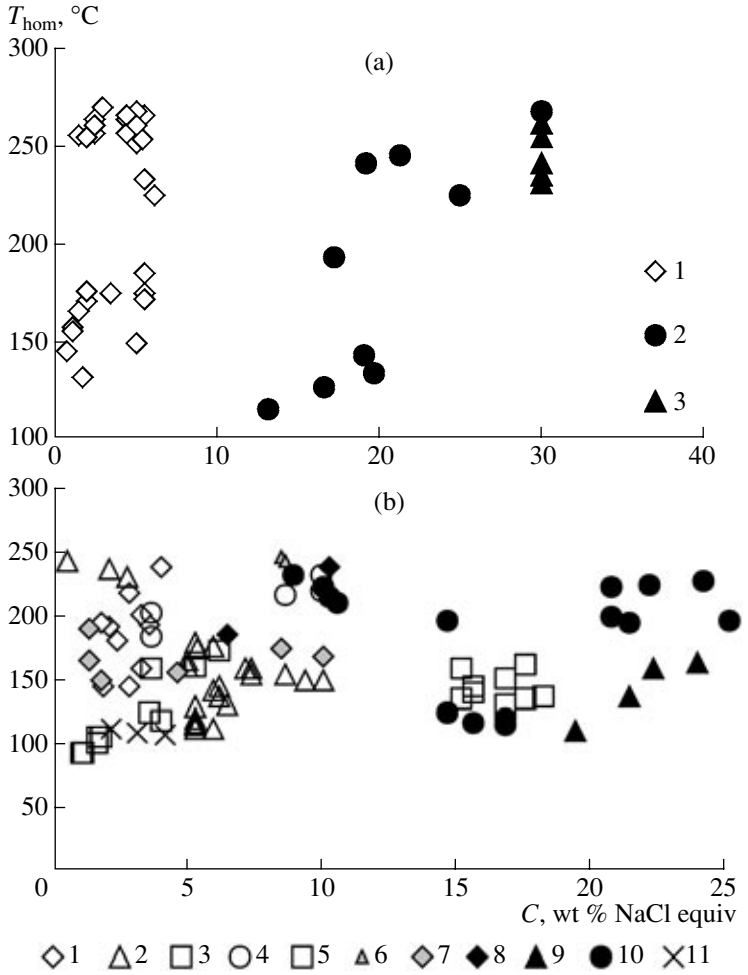

Fig. 9. Homogenization temperature versus salinity of fluid inclusions in the minerals of early (a) and late (b) stages of the Cu–Bi–Ag–Pb epithermal deposits of the Adrasman ore district. (a) (1) K-1-1, (2) K-1-2, (3) K-1-3; (b) (1) B-1, (2) K2-1P, (3) K2-1PV, (4) Sf-1P, (5) Sf-1PV, (6) Fl-1P, (7) Fl-1PV, (8) B-2, (9) K-2, (10) Sf-2P, (11) Sf-2PV.

Fluid Inclusions

Three types of fluid inclusions have been recognized from the phase composition at room temperature (Safonov *et al.*, 2000b): (1) liquid-rich inclusions; (2) vapor-rich inclusions; and (3) inclusions containing NaCl crystals. Sphalerite contains only liquid-rich inclusions. Inclusions of all three types often occur together, being confined to the same growth zones or forming randomly oriented clusters of several inclusions. Such inclusions were presumably trapped simultaneously during mineral crystallization.

Phase changes of fluid inclusions during heating and freezing are shown in Fig. 9. Fluid inclusions in the early-stage quartz (Fig. 9a) homogenize at 115–270°C, while those in the late-stage minerals (Fig. 9b) dissolve within 93–245°C. Secondary fluid inclusions found in fluorite and sphalerite from the second-stage aggregates show the same features as primary and primary–secondary inclusions. Secondary fluid inclusions in fluorite homogenize at temperatures from 150 to 190°C.

Two types of fluid inclusions were identified on the basis of ice melting and eutectic temperatures: (a) aqueous Ca–Mg chloride solution with salinity from 0.4 to 22.0 wt % NaCl equiv and (b) aqueous Mg–Na chloride solutions with salinity from 5.0 to 30.0 wt % NaCl equiv. Both solutions simultaneously occurred at the site of ore precipitation since both types of inclusions are present in the same samples. Secondary fluid inclusions are dominated by Mg–Na chloride solutions with salinity 1.0–6.0 wt % NaCl equiv. The Mg–Ca and Mg–Na fluids in early-stage minerals are lower salinity than fluids trapped by the late-stage quartz. The salinity of Mg–Ca fluid in the early-stage quartz decreases with a drop in the homogenization temperature. A similar tendency is observed for inclusions in late-stage minerals.

Syngenetic liquid-rich and vapor-rich inclusions homogenize at similar temperatures. This is considered as evidence for mineral crystallization from "boiling" fluids. A systematic decrease in salinity and homogenization temperatures suggests mixing of solutions of different salinity and temperature. A simultaneous decrease

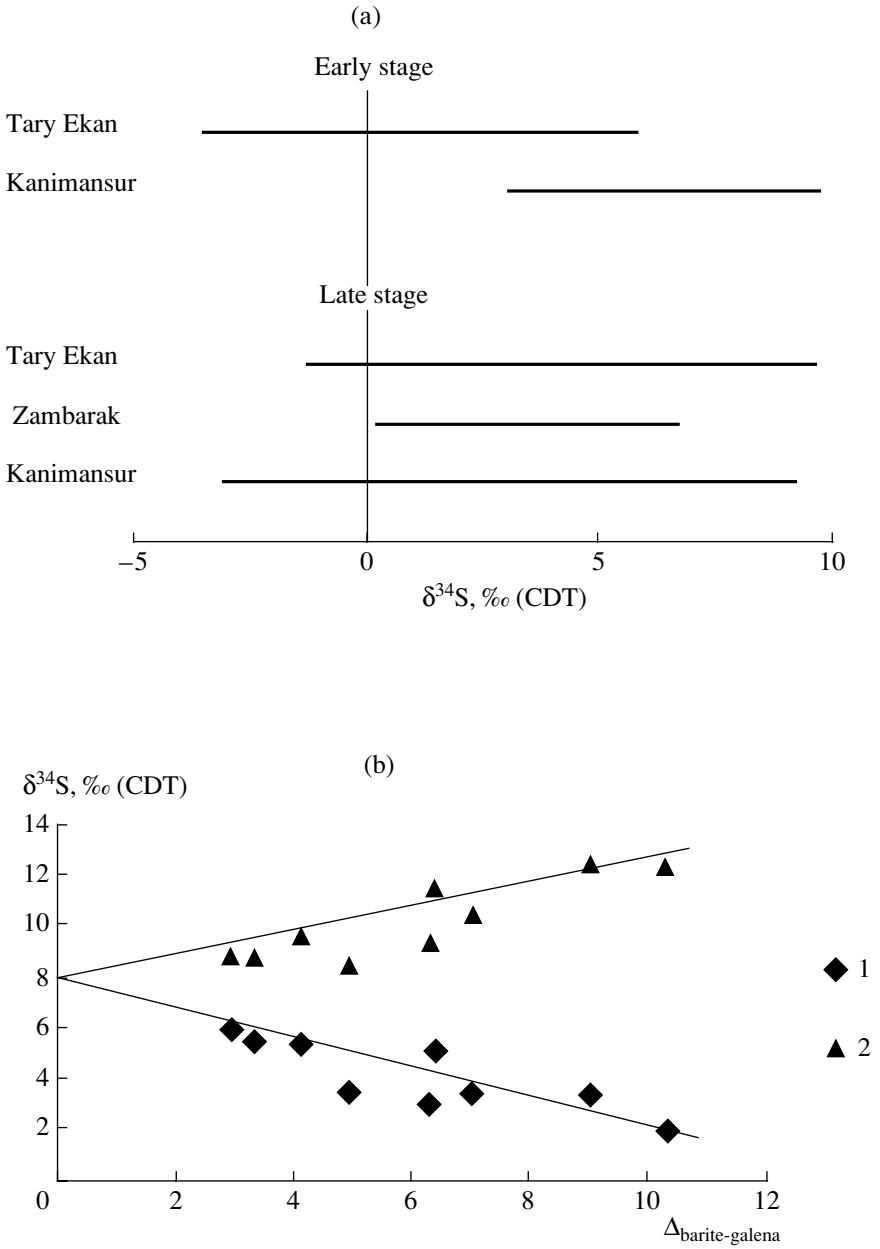

Fig. 10. Sulfur isotope compositions of the early- and late-stage minerals from deposits of the Adrasman ore district (a) and diagram (b) of $\delta^{34}S$ versus $\Delta_{PbS-BaSO_4}$ for galena (1) and barite (2) from the Cu–Bi–Ag–Pb epithermal deposits of the Adrasman ore district.

in temperature and salinity of the Mg–Na solution was presumably also caused by its mixing with lower salinity and colder (~+100°C) solution.

Sulfur and Oxygen Stable Isotpes

Sulfur isotope composition was determined in the early-stage pyrite and chalcopyrite and late-stage sphalerite, galena, pyrite, chalcopyrite, and barite. The $\delta^{34}S$ values vary from –3.6 to +9.8‰ in early sulfides and from –3.1 to +9.7‰ in the late minerals (Fig. 10a). The sulfur isotope composition in barite shows significant variations, from +8.4 to +13.8‰.

The value of $\delta^{34}S$ (+23 ± 3‰) of the mineral-forming solution was estimated from the sulfide isotope composition, ore-formation conditions, and fractionation coefficients between solid phases and solution components (Safonov *et al.*, 2000b). Fluid with such an isotope composition can be derived in the following way: acid sulfate–chloride waters formed by mixing of ground waters and SO_2, which was exsolved from a magmatic chamber, disproportionating into sulfate and sulfide S (Kiyoshu and Kurahashi, 1983). Therefore,

the hypothesis of involvement of mantle sulfur in the ore formation seems to be preferable.

The behavior of sulfur isotopes during the second stage was estimated from their fractionation between coexisting barite and galena. High (640–1450°C) temperatures calculated from the equilibrium fractionation equation unambiguously indicate isotope disequilibrium during precipitation of galena and barite. The isotopically disequilibrium sulfates and sulfides can precipitate through mixing of H_2S-rich solutions with SO_4^{2-} solutions since this process can cause both significant kinetic effects during sulfur isotope fractionation and intense precipitation of sulfates and sulfides, especially if these solutions sharply differ in temperature (Ohmoto and Rye, 1979).

The sulfur isotope composition in the mineral-forming fluid can be reconstructed from the $\delta^{34}S-\Delta_{PbS-BaSO_4}$ diagram (Fig. 10b). The intersection of lines corresponding to the isotope composition of coexisting sulfate and sulfide defines $\delta^{34}S$ of fluid if $\delta^{34}S$ and H_2S/SO_4^{2-} ratio were constant (Shelton and Rye, 1982). The obtained value is +7.5‰.

The $\delta^{18}O$ values were determined for quartz, chlorite, and hematite from the quartz–hematite–chlorite assemblage and late barite. They are from +7.5 to +13.3‰ for quartz, from –2.1 to +4.9‰ for hematite, and +7.4‰ for chlorite. The $\delta^{18}O$ values for barite are between +3.5 and +13.8‰.

The oxygen isotope composition of fluid was calculated assuming water–mineral equilibrium fractionation of oxygen isotopes using homogenization temperatures and the oxygen isotope composition determined in the same samples. The $\delta^{18}O$ values for fluid in equilibrium with quartz within 225–270°C vary from –1.5 to +1.4‰. The $\delta^{18}O$ values of quartz-forming fluid within 145–175°C vary from –4.7 to 0‰. The $\delta^{18}O$ values for fluid in equilibrium with barite at 200°C vary from –2.7 to +2.2‰. Hence, $\delta^{18}O$ in the mineral-forming fluid was 0 ± 2.5‰.

The oxygen isotope composition of the mineral-forming fluid (0 ± 3‰) is close to $\delta^{18}O$ of seawater (0 ± 2‰) and is intermediate between those of primary magmatic (from +5 to +9.5‰) and meteoric (from 0 to –10‰) waters (Sheppard, 1986). Therefore, it is difficult to determine unambiguously the fluid source. It is possible that ore-forming fluid contained both isotopically heavy meteoric water formed by exchange with host rocks and primary magmatic water (Safonov *et al.*, 2000b). The proportions of these waters were variable in different places of the precipitation site, thus causing the observed variations of oxygen isotope composition in precipitating minerals.

Based on fluid inclusion study, two fluids of different composition and density were present at the site of ore precipitation. One had a low salinity (up to 3 wt % NaCl equiv), while the other contained moderate- to low-salinity chloride solutions (up to 20–30 wt % NaCl equiv). The low-salinity fluid formed from surface waters involved in the convective cell that was induced by the magma emplacement. The fluid was enriched in H_2S with a sulfur isotope composition of 0 ± 3‰, which was extracted during filtration through volcanic rocks. This fluid is presumably close to the weakly alkaline or neutral thermal waters known in the regions of modern volcanic activity. The second fluid is an analogue of the recent acid chloride–sulfate thermal waters formed in the same areas. It was generated by interaction of gases (HCl, SO_2, H_2S, CO_2, and HF) ascending from a magmatic chamber with ground waters, the sulfur isotope composition in which during SO_2 disproportionation into H_2SO_4 and H_2S was +20‰.

Thus, the Karamazar silver–bismuth–lead–zinc epithermal deposits formed owing to input of fluids and components from different sources: low-salinity meteoric waters and high-salinity magmatic hydrothermal solutions, which extracted sulfur and carbon from host rocks.

CONCLUSIONS

The obtained data on fluid inclusions and stable isotope compositions in minerals from ore deposits that were generated by hydrothermal–magmatic systems spatially related to occurrences of plutonic and volcanic rocks indicate that ores precipitated from fluids varying from brines with salinity up to 60 wt % NaCl equiv to dilute solutions with salinity 1–3 wt % NaCl equiv. Fluids of different composition contributed to the hydrothermal–magmatic system. Orogenic (mesothermal) gold-bearing hydrothermal systems were dominated by a $H_2O–CO_2–NaCl \pm CH_4 \pm N_2$ mixture, though late-stage gold-bearing sulfosalts precipitated from an aqueous–salt fluid, which presumably formed by unmixing of an aqueous–bicarbonate protofluid. Brines played a significant role in the formation of cassiterite–silicate–sulfide and vein silver–base metal deposits. Significant amounts of CO_2 and CH_4 occurred in the fluids responsible for the formation of cassiterite–silicate–sulfide and vein silver–base metal deposits. Ore-forming fluids often sharply differ in chemical and phase composition. It was found that brine and low-density vapor-rich fluid often coexisted at the site of ore precipitation. These fluids had a different origin. They formed either owing to unmixing or boiling of the protofluid into liquid-rich aqueous–salt and vapor-rich fluids at site of ore precipitation or through fluid exsolution with formation of brines and low-density low-salinity fluid at deep levels of the hydrothermal–magmatic system. Isotope investigations showed that fluids contained components of different composition. Some of the studied hydrothermal systems (orogenic gold, tin, and vein base metal) were dominated by magmatic fluids. These fluids exsolved from granitoid magmas during crystallization. Coexistence of high-temperature (>500°C) and high-salinity (>40 wt %) fluid with melt inclusions in minerals from many ore deposits indicates that brines

exsolved from silicate melt (Candela and Piccoli, 1995; Shinohara, 1994). The formation of brines in such a way was previously called into question since exsolution of high-Cl liquid phase from silicate melt required a high Cl content in the melt owing to a high distribution coefficient. However, experimental data, as well as study of fluid and melt inclusions, confirmed the formation brine and low-density low-salinity fluid during crystallization of silicate melt (Lowenstern, 1995). Brines can form during evolution of fluid exsolved from granite magma. In this case, single-phase supercritical moderate-salinity (~8 wt % NaCl equiv) fluid or high-density liquid phase and low-salinity vapor phase exsolved (Fournier, 1987). Unmixing of low-salinity fluid generates a low-salinity vapor phase and high-salinity fluid (up to 55 wt % NaCl equiv) (Henley and McNabb, 1978; Shinohara and Hedenquist, 1997). Moderate-salinity H_2O–CO_2 fluids similar to the one that precipitated gold ores in the orogenic hydrothermal systems could form owing to magmatic activity (Ryabchikov, 1975) or dehydration and decarbonatization during metamorphism of terrigenous rocks. The presence of magmatic and metamorphic components in fluids circulating in these systems indicates their relation with magmatic activity. The emplacement of granitoid intrusions was accompanied by the exsolution of magmatic fluid and mobilization of components from host rocks owing to contact or contact–regional metamorphism (Bortnikov *et al.*, 1992).

It should be noted that some hydrothermal–magmatic systems, in particular, those forming cassiterite–silicate–sulfide and epithermal silver–bismuth–lead–zinc deposits, show input of magmatic and heated modified meteoric waters.

The high-salinity fluid is considered to exsolve from silicate melt during crystallization. The low-density fluid (2–5 wt % NaCl equiv) presumably formed in the near-surface conditions through absorption of metal-rich gases exsolved from magma into ground waters. Acid sulfate–chloride waters in the regions of recent volcanic activity are generated by interaction between ground waters and SO_2, which exsolved from a magmatic chamber and disproportionated into sulfate and sulfide S in water (Kiyoshu and Kurahashi, 1983). Magmatic and meteoric fluids also contributed to hydrothermal–magmatic systems that produced vein silver–base-metal deposits of the Verkhoyansk fold belt. The emplacement of diorite–granodiorite massifs and the existence of intermediate chambers at a depth of 15–20 km caused the introduction of metalliferous solutions from magmatic chamber, which were enriched in CO_2 and metal chloride complexes, and partial extraction of sulfur from host rocks. Subsequent lowering of ground water levels and the generation depth of the ore magmatic chamber responsible for the formation of subvolcanic granite porphyry dikes triggered convective hydrothermal cells, which promoted penetration of meteoric waters to deep levels and their heating and interaction with host rocks with formation of the ore-forming fluid.

Thus, our investigations showed that hydrothermal ores were generated from magmatic and meteoric waters circulating in hydrothermal–magmatic systems. However, high-salinity magmatic fluids played a leading role in the transportation of metals from fluid generation areas to the site of ore precipitation at most of the studied hydrothermal deposits.

ACKNOWLEDGMENTS

The author is grateful to V.Yu. Prokof'ev, G.N. Gamyanin, V.N. Sazonov, V.V. Murzin, O.V. Vikent'eva, N.N. Krivitskaya, I.A. Bryzgalov, E.Yu. Anikina, T.L. Krylova, N.V. Gorelikova, A.I. Khanchuk, V.G. Gonevchuk, and A.V. Ignat'ev for fruitful cooperation and extends additional thanks to V.Yu. Prokof'ev for providing images of fluid inclusions and original results of microthermometric investigations for diagram construction.

This study was supported by the Russian Foundation for Basic Research (project nos. 02-05-65183, 00-05-64650, 00-05-65069, 03-05-65005, 04-05-65270, and 05-05-64803) and the Division of Earth Sciences of the Russian Academy of Sciences (the program "Large and Superlarge Deposits: Location Regularities and Formation Conditions").

REFERENCES

1. E. Yu. Anikina, N. S. Bortnikov, and G. N. Gamyanin, "Rhythmical and Banded Veins at Silver–Lead–Zinc Deposits of the Kolyma–Verkhoyansk Fold Belt. Russia: Implications for Fluid Boiling," in *Mineral Exploration and Sustainable Development* (Milpress, Rotterdam, 2003).
2. A. Audetat, D. Gunther, and C.A. Heinrich, "Magmatic–Hydrothermal Evolution in a Fractionating Granite: A Microchemical Study of the Sn–W–F-Mineralized Mole Granite (Australia)", Geochim. Cosmochim. Acta **64**, 3373 (2000).
3. R. J. Bodnar, T. J. Reynolds, and C. A. Kuehn, "Fluid Inclusion Systematics in Epithermal Systems," in *Geology and Geochemistry of Epithermal Systems* (Econ. Geol, El Pasco), pp. 73–97 (1984).
4. A. S. Borisenko, "Cryometric Study of Salt Composition in Gas–Liquid Inclusions in Minerals," Geol. Geofiz., No. 8, 16–27 (1977).
5. N. S. Bortnikov, I. A. Bryzgalov, N. N. Krivitskaya, *et al.*, "The Maiskoe Multimegastage Disseminated Gold–Sulfide Deposit (Chukotka, Russia): Mineralogy, Fluid Inclusions, Stable Isotopes (O and S), History, and Conditions of Formation," Geol. Rudn. Mestorozhd. **46** (6), 475–509 (2004) [Geol. Ore Dep. **46** (6), 409 (2004)].
6. N. S. Bortnikov, G. N. Gamyanin, V. A. Alpatov, *et al.*, "Mineralogy, Geochemistry and Origin of the Nezhdaninsk Gold Deposit (Sakha-Yakutia, Russia)," Geol. Rudn. Mestorozhd. **40** (2), 137–156 (1998) [Geol. Ore Dep. **40** (2), 121 (1998)].

7. N. S. Bortnikov, A. I. Khanchuk, T. L. Krylova, *et al.*, "Geochemistry of the Mineral-Forming Fluids in Some Tin Ore Hydrothermal Systems of Sikhote Alin, Russian Far East," Geol. Rudn. Mestorozhd. **47** (5), (2005) [in press].
8. N. S. Bortnikov, V. Yu. Prokof'ev, and N. V. Razdolina, "Environment of Ore Deposition in the Charmitan Gold Vein Deposit, Nurata Mountains, Usbekistan, USSR," in *Proceedings of 29th International Geological Congress, Kyoto, Japan, 1992* (Kyoto, 1992), Vol. 3, p. 748.
9. N. S. Bortnikov, V. Yu. Prokof'ev, and N. V. Razdolina, "Origin of the Charmitan Gold–Quartz Deposit (Uzbekistan)," Geol. Rudn. Mestorozhd. **38** (3), 238–257 (1996) [Geol. Ore Dep. **38** (3), 208 (1996)].
10. N. S. Bortnikov, V. N. Sazonov, I.V. Vikent'ev, *et al.*, "Role of the Magmatogenic Fluid in the Formation of the Mesothermal Berezov Gold–Quartz Deposit," Dokl. Ross. Akad. Nauk **363** (1), 82–85 (1999) [Dokl. Earth Sci. 363 (8), 1078 (1998)].
11. N. S. Bortnikov, V. N. Sazonov, I. V. Vikent'ev, *et al.*, "The Berezovsk Giant Gold Quartz Deposit, Urals, Russia: Fluid Inclusion and Stable Isotope Studies," in *Mineral Deposits: Research and Exploration—Where Do They Meet?* (Balkema, Rotterdam, 1997), pp. 157–160.
12. N. S. Bortnikov, M. I. Stolyarov, V. V. Murzin, *et al.*, "The Svetlinsk Gold–Telluride Deposit, Urals, Russia: Mineral Paragenesis, Fluid Inclusion, and Stable Isotope Studies," *Mineral Deposits: Processes to Processing* (London, 1999), pp. 21–24.
13. T. S. Bowers, "The Deposition of Gold and Other Metals. Pressure-Induced Fluid Immiscibility and Associated Stable Isotope Signatures," Geochim. Cosmochim. Acta **55** (9), 2417–2434 (1991).
14. P. A. Candela and P. M. Piccoli, "Model Ore-Metal Partitioning from Melts into Vapor and Vapor/Brine Mixtures," in *Magmas, Fluids, and Ore Deposits*, Mineral. Assoc. Can. Short Course Ser. **23**, 101–127 (1995).
15. C. W. Field and R. N. Fifarek, "Light Stable-Isotope Systematics in the Epithermal Environment," *Geology and Geochemistry of Epithermal Systems* (Econ. Geol., El Pasco), pp. 99–128 (1985).
16. B. L. Flerov, "Tin–Base Metal Ore Mineralization of Southeastern Yakutia," in *Geology, Mineralogy of the Ore Clusters of the Yana–Kolyma Fold Belt* (YaF SO AN SSSR, Yakutsk, 1984), pp. 6–21 [in Russian].
17. R. O. Fournier, "Conceptual Models of Brine Evolution in Magmatic–Hydrothermal Systems," US Geol. Surv. Prof. Paper **1350**, 1487–1506 (1987).
18. G. N. Gamyanin, E. Yu. Anikina, N. S. Bortnikov, *et al.*, "The Prognoz Silver–Polymetallic Deposit, Sakha (Yakutia): Chemistry and Zoning of Ore Veins," Geol. Rudn. Mestorozhd. **45** (6), 531–546 (2003) [Geol. Ore Dep. **45** (6), 466 (2003)].
19. G. N. Gamyanin, E. Yu. Anikina, N. S. Bortnikov, *et al.*, "The Prognoz Silver–Polymetallic Deposit, Sakha (Yakutia): Mineralogy, Geochemistry, and Origin," Geol. Rudn. Mestorozhd. **40** (5), 440–458 (1998) [Geol. Ore Dep. **40** (5), 391 (1998)].
20. G. N. Gamyanin, N. S. Bortnikov, V. V. Alpatov, *et al.*, "The Kupol'noe Silver–Tin Deposit (Sakha Republic, Russia): An Example of the Evolution of an Ore–Magmatic System," Geol. Rudn. Mestorozhd. **43** (6), 495–523 (2001) [Geol. Ore Dep. **43** (6), 442 (2001)].
21. D. I. Groves, K. C. Condie, R. J. Goldfarb, *et al.*, "Secular Changes in Global Tectonic Processes and Their Influence on the Temporal Distribution of Gold-Bearing Mineral Deposits," Econ. Geol. **100**, 203–224 (2005).
22. D. I. Groves, R. J. Goldfarb, M. Gebre-Mariam, *et al.*, "Orogenic Gold Deposits: A Proposed Classification in the Context of Their Crustal Distribution and Relationship to Other Gold Deposit Types," Ore Geol. Rev. **13**, 7–27 (1998).
23. S. G. Hageman and K. F. Cassidy, "Archean Orogenic Lode Deposits," in *Gold in 2000*, Rev. Econ. Geol. **13**, 9–68 (2000).
24. D. O. Hayba, P. M. Bethke, P. Heald, *et al.*, "Geologic, Mineralogic, and Geochemical Characteristics of Volcanic Hosted Epithermal Precious Metal Deposits," in *Geology and Geochemistry of Epithermal Systems*, Ed. by B. R. Berger and P. M. Bethke, Rev. Econ. Geol. **2**, 129–167 (1985).
25. J. W. Hedenquist and J. B. Lowenstern, "The Role of Magmas in the Formation of Hydrothermal Ore Deposits," Nature, 519–527 (1994).
26. J. W. Hedenquist, A. Jr. Arribas, and T. J. Reynolds, "Evolution of an Intrusion-Centred Hydrothermal System: Far Southeast-Lepanto Porphyry and Epithermal Cu–Au Deposits, Philippines," Econ. Geol. **93**, 373–404 (1998).
27. C. A. Heinrich, "Geochemical Evolution and Hydrothermal Mineral Deposition in Sn (–W-Base Metal) and Other Granite-Related Ore Systems: Some Conclusions from Australian Examples," in *Magmas, Fluids, and Ore Deposits*, Mineral. Assoc. Can. Short Course Ser. **23**, 203–220 (1995).
28. R. W. Henley and A. McNabb, "Magmatic Vapor Plumes and Ground Water Interactions in Porphyry Copper Emplacement," Econ. Geol. **73**, 1–20 (1978).
29. R. Kerrich, "Mesothermal Gold Deposits: A Critique of Genetic Hypotheses," in *Greenstone Gold and Crustal Evolution*, Ed. by F. Robert, P. A. Sheahan, and S. B. Green, Geol. Assoc. Can., 13–31 (1990).
30. Y. Kiyoshu and M. Kurahashi, "Origin of Sulfur Species in Acid Sulfate–Chloride Thermal Waters, Northeastern Japan," Geochim. Cosmochim. Acta **47**, 1237–1245 (1983).
31. J. B. Lowenstern, "Applications of Silicate Melt Inclusions to the Study of Magmatic Volatiles," in *Magmas, Fluids, and Ore Deposits*, Min. Assoc. Can. **23**, 71–99 (1995).
32. S. S. Matveeva, M. Yu. Spasennykh, T. M. Sushchevskaya, *et al.*, "Geochemical Model of the Formation of the Spokoininsk Tungsten Deposit (Eastern Transbaikal Region, Russia)," Geol. Rudn. Mestorozhd. **44** (2), 125–147 (2002) [Geol. Ore Dep. **44** (2), 111 (2002)].
33. I. Ya. Nekrasov, "Primary Magmatic Zoning in Ore Deposits of North Eastern Yakutia and Its Significance for Search of Hidden Ore Bodies," in *Problems of Study and Methods of Search for Concealed Mineralization* (Gosgeoltekhizdat, Moscow, 1963), pp. 314–334 [in Russian].

34. H. Ohmoto and R. O. Rye, "Isotopes of Sulfur and Carbon", in *Geochemistry of Hydrothermal Deposits* (Willey, New York, 1979), pp. 509–567.

35. H. Ohmoto, "Stable Isotope Geochemistry of Ore Deposits," Rev. Mineral. **16**, 491–560 (1986).

36. L. M. Parfenov, "Terranes and Evolution of the Mesozoic Orogenic Belts of Eastern Yakutia," Tikhookean. Geol. **14** (6), 32–43 (1995).

37. V. Yu. Prokof'ev, N. S. Bortnikov, and L. D. Zorina, "Genetic Features of the Darasun Gold–Sulfide Deposit (Eastern Transbaikal Region)," Geol. Rudn. Mestorozhd. **42** (6), 526–548 (2000) [Geol. Ore Dep. **42** (6), 474 (2000)].

38. J. R. Ridley and L. W. Dimond, "Fluid Chemistry of Orogenic Lode Gold Deposits and Implication for Genetic Models," in *Gold in 2000*, Rev. Econ. Geol. **13**, 141–162 (2000).

39. E. Roedder, *Fluid Inclusions* (Mineral. Soc. Am., Washington, 1984).

40. I. D. Ryabchikov, *Thermodynamics of Fluid Phase of the Granitoid Magma* (Nauka, Moscow, 1975) [in Russian].

41. Yu. G. Safonov, N. S. Bortnikov, T. M. Zlobina, *et al.*, "Polymetal (Ag, Pb, U, Cu, Bi, Zn, F) Adrasman–Kanimansur Ore Field (Tajikistan) and Its Ore-Forming System. I: Geology, Mineralogy, and Structural Conditions of the Ore Deposition," Geol. Rudn. Mestorozhd. **42** (3), 195–211 (2000a) [Geol. Ore Dep. **42** (3), 175 (2000a)].

42. Yu. G. Safonov, N. S. Bortnikov, T. M. Zlobina, *et al.*, "Polymetal (Ag, Pb, U, Cu, Bi, Zn, F) Adrasman–Kanimansur Ore Field, and Its Ore-Forming System, II: Physicochemical, Geochemical, and Geodynamic Formation Conditions," Geol. Rudn. Mestorozhd. **42** (4), 350–362 (2000b) [Geol. Ore Dep. **42** (4), 317 (2000b)].

43. K. L. Shelton and D. M. Rye, "Sulfur Isotopic Compositions of Ores from Mines Gaspe, Quebec: An Example of Sulfate–Sulfide Disequilibria in Ore-Forming Fluids with Applications to Other Porphyry-Type Deposits," Econ. Geol. **77**, 1688–1709 (1982).

44. S. M. F. Sheppard, "Characterization and Isotopic Variations in Natural Waters," in *Stable Isotopes in High Temperature Geological Processes*, Rev. Mineral. **16**, 165–183 (1986).

45. H. Shinohara and J. W. Hedenquist, "Constraints on Magma Degassing Beneath the Far Southeast Porphyry Cu–Au Deposit, Philippines," J. Petrol. **38**, 1741–1752 (1997).

46. H. Shinohara, "Exsolution of Immiscible Vapor and Liquid Phases from a Crystallizing Silicate Melt: Implications for Chlorine and Metal Transport," Geochim. Cosmochim. Acta **58** (23), 5215–5222 (1994).

47. M. Yu. Spasennykh, V. M. Shmonov, T. M. Sushchevskaya, *et al.*, "Percolation of Hydrothermal Fluids through the Rocks Hosting the Iultin Deposit, Chukchi Peninsula: Evidence from the Oxygen Isotopic Composition and Rock Permeability," Geokhimiya, No. 6, 626–638 (2002) [Geochem. Int. **40** (6), 564–575 (2002)].

48. B. E. Taylor, "Magmatic Volatiles: Isotopic Variations of C, H, and S", in *Stable Isotopes in High-Temperature Processes*, Rev. Mineral. **16**, 185–225 (1986).

49. J. L. Walshe, S. W. Halley, J. A. Anderson, *et al.*, "The Interplay of Groundwater and Magmatic Fluids in the Formation of the Cassiterite–Sulfide Deposits of Western Tasmania", Ore Geol. Rev. **10**, 367–387 (1996).